Drivers of CO_2 emissions during the dry phase ~~of~~ in ~~-~~Mediterranean and Temperate ponds

Victoria Frutos-Aragón [1], Sandra Brucet [1,6,9], Rafael Marcé [2], Tuba Bucak [3], Thomas A. Davidson [3], Louisa-Marie von Plüskow [4,5], Pieter Lemmens [5,7], Carolina Trochine [1,8]

[1] Aquatic Ecology Group, University of Vic - Central University of Catalonia, Group, Vic, 08500, Spain
[2] Integrative Freshwater Ecology group, Blanes Centre for Advanced Studies (CEAB-CSIC)
[3] Department of Ecoscience, Aarhus University, Aarhus, Denmark
[4] Department ~~fish biology~~ of Fish Biology, Leibniz-Institute of Freshwater Ecology and Inland Fisheries, Berlin, Germany
[5] Laboratory of Freshwater Ecology, Evolution and Conservation, KU Leuven, Leuven, Belgium
[6] Catalan Institution for Research and Advanced Studies (ICREA), 08010 Barcelona, Spain
[7] Research Institute for Nature and Forest (INBO), Brussels, Belgium
[8] Department of Ecology, INIBIOMA CONICET, Universidad Nacional del Comahue, San Carlos de Bariloche, Argentina
[9] Fundació Privada Bionexus, 17003, Girona, Spain

Correspondence to: Victoria Frutos Aragón (victoriavfa@gmail.com)

Abstract. Pond ecosystems play an important role in the global carbon cycle with the potential to act as both sinks and sources of CO_2. However, CO_2 emissions during the dry phases of ponds remain underrepresented in global reports, despite growing evidence that climate change-driven shifts in temperature and precipitation are likely to increase the frequency and duration of these dry periods. ~~Emissions of CO₂ during their dry phases remain largely overlooked, despite growing evidence that climate change-induced shifts in temperature and precipitation will likely result in longer and more frequent dry periods~~ Here we assess CO_2 fluxes~~emissions~~ from dry pond sediments in relation to climatic region, seasonal changes, and hydroperiod duration. Specifically, we aimed to identify the key environmental drivers shaping CO_2 fluxes during the dry phase. We measured CO_2 fluxes~~emissions~~ from bare air-exposed sediments using closed static chambers equipped with internal mini-loggers in 30 ponds across Mediterranean and Temperate regions. Ponds acted as sources of CO_2 during dry phases, with emissions ranging from 127 to 4889 mg C m^{-2} d^{-1} (mean ± SD = 1398 ± 1201). Although mean emissions did not differ significantly between climate regions, hydroperiod length interacted with climate and season, showing a significant effect in summer, particularly in Mediterranean ponds, where longer hydroperiods led to higher emissions. Emissions were considerably higher in summer than in autumn, primarily driven by the interaction between sediment temperature and water content. The highest fluxes occurred at approximately ~~c.~~ 27 ºC and sediment water content between 27% and 44%. Additionally, ponds in better conservation status and with lower carbonate content emitted more CO_2. Our findings improve understanding of CO_2 emissions during increasingly common dry phases and highlight how climate modulates local sediment conditions, thereby influencing the magnitude of these emissions. This underscores the need for comprehensive assessments of carbon fluxes that incorporate dry-phase emissions, accounting for climate, hydroperiod, and both direct and indirect effects of local environmental drivers.

1 Introduction

Inland waters play a fundamental role in the global carbon cycle by processing substantial amounts of organic carbon from terrestrial ecosystems, which ~~that~~ can be buried, exported, or released to the atmosphere as CO_2 and CH_4 (Cole et al., 2007; Raymond et al., 2013; Tranvik et al., 2009). Among these systems, ponds are globally abundant ecosystems (Verpoorter et al., 2014). Despite covering a small fraction ~~portion~~ of Earth's surface, they exhibit intense biogeochemical processes compared to ~~with~~ other freshwater systems (Holgerson and Raymond, 2016; ~~Verpoorter et al., 2014~~). Ponds' CO_2 emissions per unit area can be comparable to those of larger freshwater bodies and upland soils (Downing, 2010; Hill et al., 2021; Obrador et al., 2018; Oertli et al., 2009). However, reported CO_2 emissions from ponds are highly variable, ranging from hundreds to several thousand mg C m^{-2} d^{-1}. For instance, ponds of similar size (< 0.001 and 0.001–0.01 km^2) reported by Holgerson and Raymond (2016) emitted on average 254 and 422 mg C m^{-2} d^{-1}, respectively, whereas exposed pond sediments reported by Keller et al. (2020) range from -73 to 11765 mg C m^{-2} d^{-1}.

This significant variability in reported CO_2 fluxes underscores the importance of key factors influencing greenhouse gas (GHG) emissions, such as drying events, which can range from partial water level reductions to complete desiccation (Fromin et al., 2010). ~~One key factor influencing greenhouse gas (GHG) emissions from inland waters is drying events, which may range from partial water level reductions to complete desiccation (Fromin et al., 2010)~~ Drying events are a common feature experienced by many freshwater systems (Gao et al., 2025; Prananto et al., 2020). Globally, up to 40% of inland waters are considered non-permanent (Pickens et al., 2020), and they are particularly prevalent in arid or semi-arid regions such as the Mediterranean (Sánchez-Carrillo, 2009). The shift between wet and dry phases creates fluctuating anaerobic and aerobic conditions, which ~~affects~~ affect carbon cycling, particularly CO_2 and CH_4 dynamics (Downing, 2010; Rulík et al., 2023; Zhao et al., 2020; Zou et al., 2022). As a result, CO_2 can dominate the total carbon emissions during dry periods while limiting CH_4 (Beringer et al., 2013; Zou et al., 2022).

During wet phases, ponds can act as either sources or sinks of atmospheric CO_2, having the potential to store substantial amounts of organic carbon (DelVecchia et al., 2021; Taylor et al., 2019). CO_2 fluxes are primarily regulated by diffusion, while ~~its~~ their accumulation is controlled by the carbonate buffering system (Cole and Caraco, 1998). In contrast, during dry periods, ~~hases~~ ponds may be sources of CO_2 because the absence of a water column facilitates CO_2 diffusion from exposed sediments, frequently resulting in increased emissions (Beringer et al., 2013; Catalán et al., 2014; Gilbert et al., 2017; Obrador et al., 2018) ~~as the absence of a water column facilitates CO₂ diffusion from exposed sediments, frequently resulting in increased emissions (Beringer et al., 2013; Catalán et al., 2014; Gilbert et al., 2017; Obrador et al., 2018)~~. Consistent with these patterns, global comparisons by Zou et al. (2022) and Keller et al. (2020) revealed that CO_2 emissions were lower during ~~the~~ wet phases than ~~the~~ dry phases across temporary inland water ecosystems (streams, reservoirs, wetlands, lakes, and ponds) spanning various climate regions. Particularly, ponds exhibited the highest sediment-driven emissions across inland freshwater ecosystems (Keller et al., 2020).

Previous studies suggest that CO_2 emissions from ponds during the dry phases are ~~largely governed~~ primarily governed by the same drivers that regulate emissions in natural soils and other aquatic environments (Håkanson, 1984; Keller et al., 2020; Martinsen et al., 2019; Oertel et al., 2016). The primary source of CO_2 efflux is the biological activity on organic matter in the sediments. Increased ~~Higher~~ oxygen availability, during dry conditions stimulates enzymatic activity and microbial degradation of organic matter by bacteria and fungi, enhancing CO_2 release (Fromin et al., 2010). Local factors strongly influence this process, primarily depending on sediment temperature, sediment water content, and organic matter concentration (Agnew et al., 2021; Fraser et al., 2016; Jarvis et al., 2007; Lloyd and Taylor, 1994; Pozzo-Pirotta et al., 2022; Suh et al., 2009). Additionally, the composition of organic matter (e.g., humic-like components) further affects the CO_2 emissions (Catalán et al., 2014; Obrador et al., 2018). Other edaphic factors, such as porosity, structure, bulk density, pH, and the chemical and biological characteristics, can also modulate the CO_2 emissions (Buragienė et al., 2019). Among biological components, macrophytes influence CO_2 emissions by altering sediment conditions and microbial activity (Baastrup-Spohr et al., 2016; Tak et al., 2023; Weise et al., 2016). They contribute nutrients and organic compounds, including fulvic acids, which are readily decomposed by microorganisms, thereby enhancing the respiration and decomposition of organic matter (Bottino et al., 2021; Wang et al., 2017).

~~In addition, r~~Regional meteorological conditions, such as air temperature and precipitation, strongly influence ~~the local and edaphic factors linked to CO₂ emissions, which~~local and edaphic factors linked to CO_2 emissions. These emissions respond sensitively to changes in sediment temperature (cold–heat) and water content (drought–excess water) (Fromin et al., 2010; Unger et al., 2010). Rewetting of previously dry soils, driven by precipitation, can trigger a rapid increase in microbial activity and ~~subsequent~~ CO_2 release. This ~~, a~~ phenomenon is known as the "Birch effect" (Fromin et al., 2010; Jarvis et al., 2007). In addition, land use and conservation status can indirectly affect emissions by modifying nutrient loading in sediments and the inflow of organic matter (Bartrons et al., 2025; Novikmec et al., 2016). These factors are ~~factors~~ known to affect emissions during the wet phase (Bhushan et al., 2024; Morant et al., 2020). However, their potential role in shaping emissions during the dry phase remains largely underexplored.

The combined effects of climate change, land-use and water abstraction are likely to intensify the frequency and severity of drying events in regions worldwide, including central Europe and the Mediterranean region (Burkett and Kusler, 2000; Dimitriou et al., 2009; IPCC, 2014; Oroud, 2024; Pekel et al., 2016; Voudouri et al., 2023; Williams et al., 2010). In this context, it is especially concerning that the dry phases of temporary inland water bodies are often excluded in GHG studies, which tend to focus predominantly on wet periods, overlooking the significant role that dry sediments can play in carbon cycling (Marcé et al., 2019). This knowledge gap likely underestimates the impact of hydrological dynamics, severely limiting our understanding of the key drivers of CO_2 emissions during the dry phases (Hanson et al., 2015; Keller et al., 2020; Premke et al., 2016). Furthermore, the sequence and duration of wet and dry periods can create ecological and biogeochemical feedbacks, where the length of each phase influences the next, thereby modulating carbon processing, macrophytes development, and greenhouse gas emissions throughout the hydroperiod (Girard et al., 2024; Jin et al., 2023).

For this reason, our study aims to address this gap by identifying the main drivers of CO_2 fluxes during dry periods and examining how the preceding wet phase, in terms of hydroperiod length (i.e., the duration of water presence prior the dry phase in a pond throughout the year,) influence them, through a comparison of ponds from contrasting climatic regions across two seasons.

Here, we quantified CO_2 fluxes from air-exposed pond sediments during the dry phase across different seasons (summer and/or autumn) in 30 ponds with varying hydroperiod lengths, located in Mediterranean and Temperate climate regions. Within this environmental and biogeochemical framework, we aimed to identify the key drivers regulating CO_2 emissions from dry pond sediments.

Specifically, we asked: (1) How do seasonal and climatic differences influence CO_2 fluxes from pond sediments during the dry phase?; (2) To what extent do climate and hydroperiod length affect CO_2 emissions under dry conditions?; (3) Which local sediment and environmental variables, including possible indirect factors, best explain variation in CO_2 fluxes across ponds?; (4) Does macrophyte coverage, potentially reflecting conservation status, influence CO_2 emissions during the dry phase?.

Based on these questions, we hypothesized that:

(1) CO_2 fluxes from sediments during the dry phase will vary across seasons and climate regions, with higher emissions in summer due to enhanced microbial activity and organic matter decomposition; (2) climate and hydroperiod length will influence CO_2 emissions, with shorter hydroperiods (ponds that are inundated for shorter periods) leading to lower emissions due to reduced sediment water content and organic matter availability; (3) local sediment conditions such as temperature, sediment water content, and organic matter will primarily drive emissions, while climate sets broader seasonal and hydrological patterns; and (4) ponds with larger macrophyte coverage, reflecting better conservation status (e.g., clear water with turbidity < 5 NTU, extensive native emergent vegetation, and ≥ 50% hydrophytic plant cover, particularly vascular submerged species or charophytes covering > 75% of the pond bottom), will exhibit greater CO_2 emissions due to increased vegetation senescence during the dry phase.

2 Methodology

2.1 Pond selection and data collection

We collected data from 30 ponds across four countries in Europe distributed in two climate regions, Temperate (N = 14) (Belgium, Denmark and Germany) (Fig. 1a) and Mediterranean (N = 16) (Spain) (Fig. 1b), spanning latitudes from 41° 49' 9" to 54° 54' 8" N and longitudes from 2° 21' 7" to 14° 21' 9" E (Table A1).
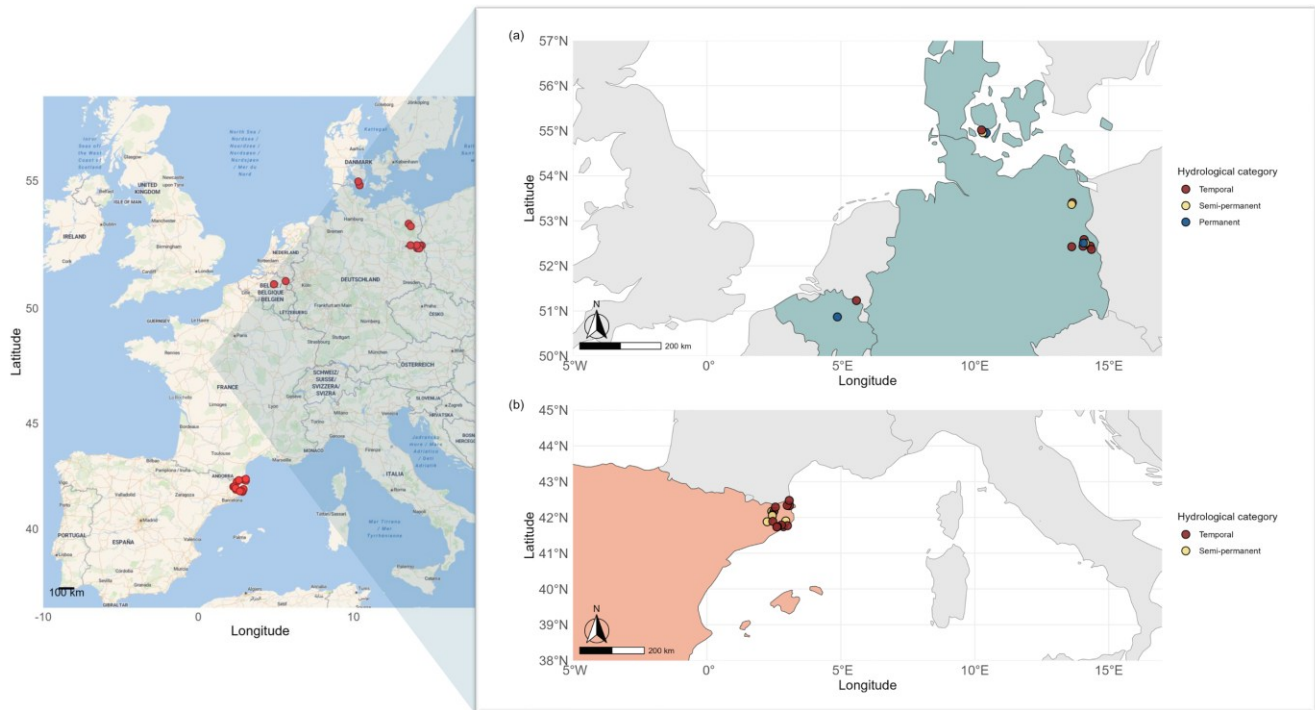
Figure 1: Geographic locations of the studied ponds. Left panel: map created using Stadia Maps outdoors basemap and OpenStreetMap data. Map data © OpenStreetMap contributors, © Stadia Maps (https://stadiamaps.com/). Ponds are highlighted in red. Right panel: map showing ponds categorized by hydroperiod: temporary (dark red), semi-temporary (yellow), and permanent (dark blue). Countries are colour-coded according to their climate regions: Mediterranean (orange) and Temperate (light blue).

Our study included 20 temporary, 5 semi-permanent, and 3 permanent ponds. Temporary ponds dried completely every year, semi-permanent ponds dried some years (including the sampling year), and permanent ponds never fully dried. ~~Our set of selected ponds included 20 temporary ponds (dry out completely every year), 5 semi-permanent ponds (dry out during some years – including the year of the sampling – but not every year) and 3 permanent ponds (never completely dry out but experienced pronounced drops in water level during the sampling year).~~ We based this classification on hydrological information obtained from field monitoring and logger data collected between 2021 and 2023. During 2022 (the sampling year), these ponds either dried out or experienced significant water level declines (e.g., permanent ponds), ~~exposing~~ large areas of the pond basin sediments to air (on average, $84 \pm 20\%$ of the total pond area). All ponds were in lowland rural areas below 800 m elevation, spanning diverse land uses such as cattle-grazing lands, agricultural fields, and protected nature reserves (López-de Sancha~~,~~ et al., 2025). The selected ponds covered a wide range of hydro-geomorphological and sediment characteristics (Table A2~~1~~). We measured CO_2 ~~dry~~ fluxes from exposed bare sediment during summer (N~~n~~= 23) and/or autumn (N~~n~~= 23), including ponds in one or both seasons, depending on the timing and extent of their water level decline.

We used a combination of regional and local factors to characterize the ponds and their surrounding landscapes, aiming to identify the main drivers of dry sediment CO_2 fluxesemissions (Table A32):

2.2 Environmental and landscape variables

2.2.1 Climatic regional data

150   We used temperature (40-year mean of annual temperatures (1978-2018) and the annual mean for 2022) and precipitation (40-year mean annual precipitation (1978-2018) and the annual mean for 2022) calculated from the nearest cell 1 X 1 km to each pond from the fifth generation of ECMWF atmospheric reanalysis of the global climate (ERA5) Copernicus Climate Change Service (C3S) (Wouters, 2021). We used long-term climatic averages (1978-2018) to represent the average climatic condition in the region, and the mean annual values for 2022 to capture the exceptional heat and drought conditions during

155   the sampling year.

2.2.2 Hydrological data

We defined hydroperiod length as the number of months with surface water present during the 12 months preceding the final sampling (autumn), representing the duration of the preceding wet phase. We used hydroperiod length because it is a simple, easily obtained metric that indirectly integrates a suite of biotic and abiotic processes occurring during the preceding wet

160   phase, such as carbon processing and macrophyte development. We estimated hydroperiod length using temperature data (HOBO U2OL-0X, Onset Brands) and/or water level loggers (Cera-Diver, Schlumberger). The water level loggers operate based on differential pressure measurements, enabling the detection of water presence. For temperature-based assessments, we deployed two loggers: one outside the pond and another at its maximum depth. The pond was considered dry when the recorded temperatures from both sensors coincided, indicating exposure of the deepest zone. We measured the pond depth

165   profile *in situ* along two perpendicular transects at 2 m intervals using a graduated pole perpendicular to the base ground of the pond, to calculate the maximum depth. We included maximum depth in the models to assess whether this geomorphological trait (shallowness) could indirectly influence CO_2 emissions under dry conditions. Pond areas were delineated through manual polygon digitization in Google Earth Pro (Google LLC, 2021), enabling georeferenced surface area calculations suitable for spatial ecological analysis.

170   ### 2.2.3 Water physicochemical data

We measured physicochemical parameters and chlorophyll a during the preceding wet phase (spring) and used them as proxies for the ponds' trophic status. We determined total nitrogen (TN) and total phosphorus (TP) concentrations (mg L^{-1}) from unfiltered water samples (250 ml) following Sen Gupta and Koroleff (1973). We measured dissolved organic matter (DOC) in mg L^{-1} after filtering water samples through pre-combusted GF/F filters (0.7 μm pore size), using a TOC-L

analyzer (TOC-L, Shimadzu). We measured chlorophyll a (µg L^{-1}) using an Algae fluorometer (AlgaeTorch, bbe Moldaenke). For more detailed information, see Bartrons et al. (2025).

2.2.~~3~~4 Landscape data

We classified six land-use types: open nature, forest, pasture, arable, grassland and urban. Land use was assessed within 5 m and 100 m radii from each pond. We estimated the percentage cover of each land-use type based on visual field observations beyond these radii.

2.2.~~4~~5 Conservation data

We calculated the ECELs index (Ecological Conservation of Ephemeral Lentic Systems~~,~~ (Sala et al., 2005)) as a measure of pond conservation status. This index is based on five main components of the pond: pond morphology (e.g., littoral slope, burial, impermeabilization), human impacts around the pond (e.g., infrastructure, nearby land uses, protected area), water aspects (e.g., transparency, odour), emergent vegetation (e.g., perimeter and in-pond cover, dominant community), and hydrophytic vegetation (e.g., submerged or floating vegetation). This index ranges from 0 to 100, with higher values indicating better pond conditions. In this study, we analyzed a subset of ECELS values previously reported in López-de Sancha et al. (2025a; 2025b) to assess their potential relationship with CO_2 emissions during the dry phase.

~~2.2.3 Water physicochemical data~~

~~We measured physicochemical parameters and chlorophyll a during the preceding wet phase (spring) and used them as proxies for the ponds' trophic status. We determined total nitrogen (TN) and total phosphorus (TP) concentrations (mg/L) from unfiltered water samples (250 ml) following Sen Gupta and Koroleff, (1973). We measured dissolved organic matter (DOC) after filtering water samples through pre-combusted GF/F filters (0.7 µm pore size), using a TOC-L analyzer (TOC-L, Shimadzu). We measured chlorophyll a using an Algae fluorometer (AlgaeTorch,bbe Moldaenke). For more detailed information, see Bartrons et al. (2025).~~

2.2.6 Macrophyte data

We measured macrophytes coverage *in situ* as the percentage of the pond's area covered by emerged vegetation. We also calculated macrophytes PVI (Plant Volume inhabited) as the percentage of water volume occupied by macrophytes (submerged, floating, and emergent) in the pond.

2.3 CO₂ dry flux~~es~~ measurements

We measured CO_2 fluxes~~emissions~~ from the surface sediment using closed static chambers in a total of 30 ponds during summer (July--August) and/or autumn (September~~October~~--November) ~~of~~ 2022. Measurements were conducted once per season at each pond during daytime (08:00–19:00 h), with no temporal replicates within the same season (Table A1; S1~~2~~).

205 CO$_2$ fluxes were measured by monitoring concentration changes over time using mini-loggers placed in static chambers. The chambers consisted of opaque polypropylene buckets covered with aluminium tape to minimize solar warming of the headspace. Each chamber had an internal volume of 8 L (diameter 345 mm; height 160 mm) and enclosed a sampling area of 0.075 m². The mini-loggers inserted in the chambers were built following the methodology described by Bastviken et al. (2015). We used a CO$_2$ sensor module (SCD30, Sensirion) to log CO$_2$, temperature, and humidity every 2-4 seconds. The

210 sensor was connected to an electronic circuit~~ry~~ board~~,~~ (Mega250, Arduino or Uno, Arduino) equipped with a real-time clock, an SD card for data storage, and powered by an external battery (RS PRO Q2). The chamber had ~~inside~~ a small fan inside at the top to recirculate the air and prevent stratification, but there was no airflow through the chamber.

To account for the heterogeneity of the pond basin, we selected between four and eight spots in each pond, depending on its size, to measure the CO$_2$. The chambers were placed on bare sediment and fitted to plastic collars inserted approximately 1

215 cm into the soil to minimise lateral gas leakage. ~~At the remaining spot, we performed a 1-hour measurement. In the latter case, we additionally took manual gas samples (using a syringe and vacuum Exetainer® vials) every ten minutes. We processed these samples by gas chromatography (Agilent 8890 GC system with a PAL RSI 120 autosampler; CTC Analytics, Switzerland; (Petersen et al., 2012)~~. We measured CO$_2$ fluxes for 5 minutes at all spots in each pond, with a 5-minute flushing interval. At one spot per pond, we conducted a 1-hour closing time measurement using the same internal

220 CO$_2$ sensor. Logger data and integration were comparable to the 5-minute ~~During~~measurements. During the 1-hour measurement, we collected six 10 mL manual gas samples every 10 minutes (using a 60 mL syringe, BD Plastipak, and 5.9 mL vacuum Exetainer® vials, Labco) to assess the reliability of sensor-based measurement.

The CO$_2$ sensors ~~provide data in ppm units, and~~were pre-calibrated by the manufacturer (Sensirion AG, 2020) and provided data in ppm units. The sensors were configured following manufacturer recommendations, including forced recalibration (we

225 used 410 ppm), altitude compensation (60 m), atmospheric pressure compensation (1000 mbar), and a fixed measurement interval, ensuring stable operation across deployments. Measured concentrations were corrected for water vapour using the simultaneously recorded temperature and relative humidity data. ~~calibration was not required~~To calculate CO$_2$ fluxes, we applied a 3-point rolling average to the raw data to reduce background noise. The initial 1-2 minutes of each measurement period were excluded due to increased signal noise likely caused by humidity and temperature fluctuations immediately after

230 chamber closure. Flux values were then derived from the data corresponding to the last 2-3 minutes of each 5-minute measurement period to ensure more accurate linear flux estimates (Johannesson et al., 2024). For the 1-hour measurements, the same approach was applied but using longer time intervals within each recording to obtain the linear fit. The CO$_2$ flux was calculated by the ideal gas law ~~,~~using the following Eq. (1)) (~~:~~Podgrajsek et al., 2014):

$$F_{dif} = \left(\frac{\Delta C_i}{\Delta t} \cdot \frac{P \cdot M}{R \cdot T} \cdot \frac{Vi}{Ai} x\ 1000 \right) x\ (60\ x\ 60\ x\ 24) \tag{1}$$

235 Where F_{dif} represents the diffusive flux (mg C m^{-2} d~~h~~$^{-1}$), $\frac{\Delta C_i}{\Delta t}$ is the change in gas concentrations (ppm·10^{-6}), P is the atmospheric pressure (atm), R is the gas constant (L·atm/mol·K), T is the temperature (K), M is the molar mass of carbon (g

mol^{-1}), Vi is the volume of the chamber (L), Ai is the area of the chamber (m^2). The factor of 1000 accounts for the unit conversion from grams to milligrams, and the multiplication 60 x 60 x 24 accounts for the conversion from seconds to days. The measurement approach used in this study follows Bastviken et al. (2015), who provide detailed information on logger preparation, sensor evaluation, calibration, and data processing in their manuscript and supplement.

2.4 Sediment characterisation

After measuring CO_2, we collected sediment samples from the upper 5 cm of the surface layer and recorded temperature (°C) in situ using a portable soil probe thermometer (30.1033, TFA Dostmann). In the laboratory, we measured pH (HI 98127, HANNA) and conductivity (BiXs50, Violab), in μS cm^{-1} at 25 °C in a 1:2.5 sediment: ultrapure water (Milli-Q) mixture. Sediment water content (%) was determined as weight loss after drying 5 g of fresh homogenized sediment at 105 °C furnace muffle (Carbolite Gero, CWF 12/13) for 48h. Organic matter (%) and carbonate content (%) in the sediments were determined through sequential loss on ignition, in the muffle furnace and expressed as percentages of the dry sediment weight. Samples were combusted in a muffle furnace (Carbolite Gero CWF 12/13) at 500 °C for 4 hours to estimate organic matter content, followed by combustion at 950 °C for 2 hours to assess mass loss associated with carbonates, commonly used as a proxy for carbonate mineral content (Heiri et al., 2001; Martinsen et al., 2019). We assessed sediment texture using a hand-texturing method, categorized samples on the dominant material, and grouped them as clay, loamy or sandy (Thien, 1979).

2.4.1 Dissolved organic matter characterization

To assess the composition of organic matter in sediments, we extracted the water-extractable organic matter (WEOM) in a 1:40 sediment water ratio (p/p) following Obrador et al. (2018). We used the solutions obtained from WEOM to determine the dissolved organic carbon (DOC) and characterized dissolved organic matter (DOM) in the sediment. We analyzed DOC using a TOC analyzer (TOC-VCS, Shimadzu) and expressed the results as mg C g^{-1}. We characterized DOM using absorbance and fluorescence spectroscopy to gain insights into the composition, origin, and reactivity of sedimentary organic matter. We obtained the UV-Vis absorbance spectra (200–800 nm) using a UV-Vis spectrophotometer (Cary 4000, Agilent) and fluorescence excitation-emission spectra using a fluorescence spectrophotometer (F-700, HITACHI). From DOM characterization, we calculated several absorbance and fluorescence indices: 1) the humification index (HIX; unitless), which indicates the degree of organic matter humification, as the ratio of the fluorescence emission peak areas between 435–480 nm and 300–345 nm at an excitation wavelength of 254 nm. 2) The biological index (BIX; unitless), which reflects the autochthonous productivity and freshness, as the ratio of the fluorescence intensities between 380 and 430 nm at an excitation wavelength of 310 nm (Fellman et al., 2010; Gabor et al., 2014; Huguet et al., 2009). 3) The fluorescence index (FI; unitless), used to assess the proportion of autochthonous versus allochthonous organic matter, as the ratio of emission intensities between 4750-500 nm at an excitation wavelength of 370 nm. 4) Specific ultraviolet absorbance (SUVA; L mg^{-1} m^{-1}), an indicator of aromaticity, calculated by dividing the UV coefficient absorbance at 254 nm by the DOC concentration

(mg /L^{-1}) (Weishaar et al., 2003). 5) Absorbance at 254 nm, indicating the presence of aromatic organic compounds and used to assess the quantity and complexity of DOM. 6) Absorbance at 300 nm, reflecting the amount of less complex and more biodegradable organic compounds.

We further analyzed the DOM fluorescence properties using parallel factor analysis (PARAFAC) following Murphy et al. (2013). Multiple models were evaluated to determine the optimal number of components, based on split-half analysis validation, core consistency, model fit, and residual examination. We used the Openfluor.org pPlatform to identify fluorescent components by matching excitation and emission spectrum spectra to models in the repository, with a Tucker Congruence Coefficients (TCC) accuracy of 0.99 . (Table S2).

We processed DOM and PARAFAC data using the R package StaRdom (Pucher et al., 2019). Further methodological details and processing steps are available in the supplementary material.

2.5 Statistical analysis

We used the non-parametric Mann–Whitney test (Wilcoxon rank-sum test) to compare overall CO_2 fluxes across climates (Mediterranean, Temperate) and seasons (Summer, Autumn) (Hypothesis 1)We used analysis of variance (ANOVA) to compare overall CO_2 emissions across climates (Mediterranean, Temperate) and seasons (Summer, Autumn) (Hypothesis 1), based on the average of multiple measurements in each pond (wilcox_test function in rstatix package (Kassambara, 2023)). Before analysis, data were assessed for normality using Shapiro–Wilk tests (shapiro.test function in stats package (R Core Team, 2024)). To assess whether our results significantly differed from published values of pond dry fluxes, we conducted Welch's t-tests (t.test function in stats package) based on summary statistics (means, standard deviations, and sample sizes). To investigate the influence of hydroperiod length on CO_2 fluxesemissions, we applied a linear mixed-effects model (LMM) (lmer function in lme4 package (Bates et al., 2015)). This model tested whether the slopes and intercepts describing the relationship between hydroperiod length and CO_2 emissions differed significantly between climates and seasons. Pond ID was included as random effect (Bolker et al., 2009), with CO_2 emissions as the response variable and hydroperiod length, season, and climate as the fixed effects. We calculated marginal and conditional R-squared values for the models (r.squaredGLMM function in MuMIn package (Bartoń, 2023)). To evaluate the significance and direction of the effect of hydroperiod length within each climate and season, we extracted the estimated slopes and their 95% confidence intervals (CI) from the model (emtrends function in emmeans package (Lenth, 2025)). This approach allowed us to assess how the effect (slope) of hydroperiod length on CO_2 emissions varied across seasons and climate regions (Hypothesis 2). Then, to identify the main drivers of fluxesemissions across climate regions, seasons and hydroperiod (Hypotheses 3 and 4), we used Generalized Linear Mixed Models (GLMMs) using a Gaussian distribution. For these analyzes, we treated all subsamples as individual observations in the GLMMs, including Pond ID as a random intercept to account for nested data structure. We normalized all numeric variables (predictors and response) using Ordered Quantile (ORQ) normalization

(orderNorm function in bestNormalize package (Ryan A. Peterson, 2021)), a one-to-one transformation that transforms values into a vector that follows a Gaussian distribution (Peterson and Cavanaugh, 2020).

We assessed correlations among predictor variables (Table A3~~2~~) using Pearson's correlation (Cor function in corrplot package (Wei and Simko, 2024)), retaining variables with low multicollinearity ($|r| < 0.6$) as fixed effects in the GLMMs. We fitted GLMMs (glmer function in lm4 package (Bates et al., 2015)), with CO_2 fluxes~~emissions~~ as the response variable and Pond ID as a random intercept (Bolker et al., 2009). We also tested biologically relevant interactions, including the one between sediment temperature and sediment water content (Fig. S1). To capture the nonlinear relationship between sediment water content and CO_2 fluxes~~emissions~~, we included second-degree polynomial terms (using orthogonal polynomials) (poly function in stats package~~-~~) in our GLMMs (Fox, 2003). This approach allowed us to model both the linear and quadratic effects of sediment water content on CO_2 fluxes~~emissions~~ while minimizing multicollinearity. We used multi-model inference, an automated model selection (dredge function in MuMIn package) to identify the best models based on Akaike's Information Criterion (AIC) (Akaike, 1998). We calculated marginal and conditional R^2~~-squared~~ values for the models (r.squaredGLMM function in MuMIn package). While p-values, coefficients, and standard errors of fixed effects were obtained directly from the model (sjPlot package (Lüdecke, 2021)). We applied a four-step filtering approach to select the final models. First, we retained models in which all predictor variables were statistically significant ($p < .05$). Second, we assessed multicollinearity using the Variance Inflation Factor (VIF) (vif function in car package (Weisberg and Fox, 2011)), ensuring that all variables included had VIF < 5. Third, we evaluated the model fit and validity using residual diagnostics (TestDispersion and testUniformity ~~function~~ functions in DHARMa package (Hartig, 2022)). This last step included assessing homoscedasticity, normality, and the absence of overdispersion or spatial autocorrelation in the residuals. Finally, we selected the model with the lowest AIC value (Akaike, 1998).

All statistical analyses were performed using R ~~studios~~ Studio software version 4.4.2 (R Core Team, 2024). We used the ggplot 2 R package (Wickham, 2016) to create the plots ~~-~~ and ggmap R package for maps (Kahle and Wickham, 2013) and Visreg for partial plots of GLMMs (Breheny and Burchett, 2017).

3 Results

Our study showed that ponds were on average ~~overall~~ sources of CO_2 to the atmosphere during the dry period, with CO_2 sediment emissions ranging from 127 to 4889 mg C m^{-2} d^{-1} (mean ± SD: 1398 ± 1201, median = 1078, $N = 30$). However, we also recorded some negative values indicating localized CO_2 uptake from the atmosphere, accounting for about 4% of the total fluxes measured.~~.~~ CO_2 fluxes~~emissions~~ exhibited high variability both among ponds and within ponds (Fig. 2; Table S1~~2~~).
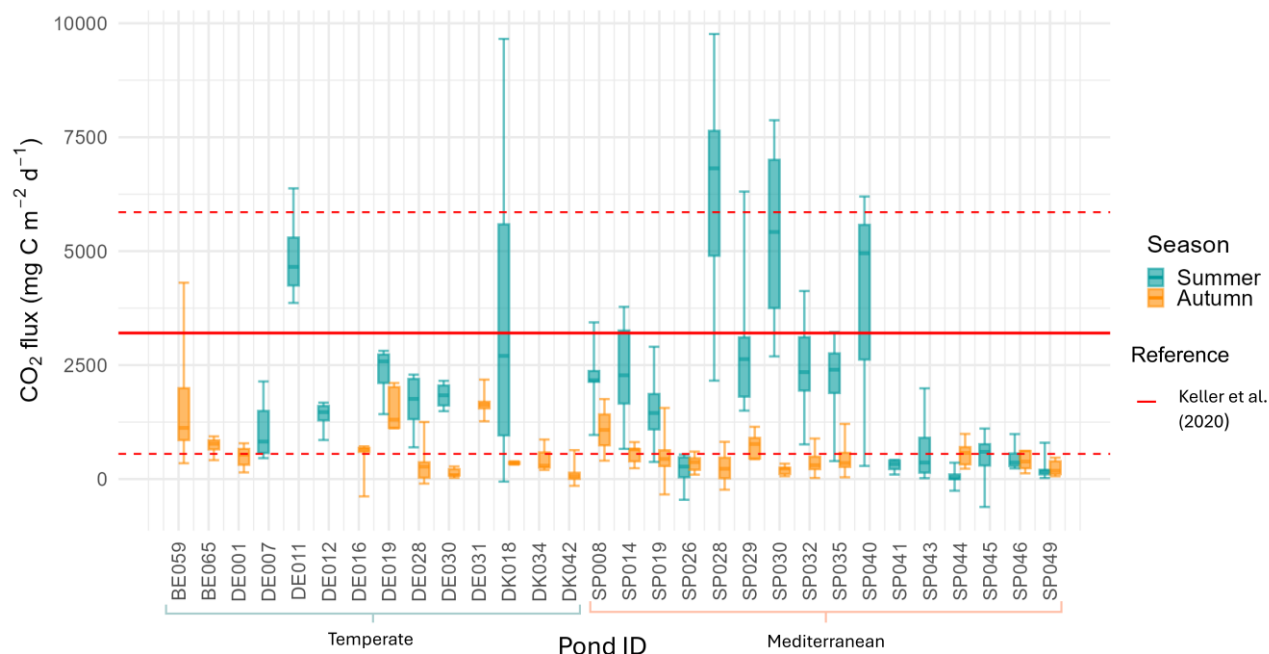
330   **Figure 2~~1~~. Boxplots of CO₂ fluxes for each pond in summer and autumn. Boxes represent the interquartile range with the median indicated by a solid line; outliers are shown as individual points. The red lines indicate the CO₂ fluxes reported by the study on dry flux~~es~~ ~~emission~~ on ponds by Keller et al. (2020), the red solid line indicates the mean, and the red ~~d~~ashed lines represent the standard deviations. Pond IDs are grouped using brackets according to their Climate region (Temperate or Mediterranean). The first two capital letters indicate the country initials (see Table A1).**

335   ~~Table 2. Summary CO₂ fluxes by season. For each pond, the table shows the mean ± standard deviation (SD) of CO₂, as well as the observed range (minimum to maximum) values.~~

			~~CO₂ fluxes (mg C m⁻² d⁻¹)~~					
			~~Summer~~			~~Autumn~~		
~~Pond~~	~~Country~~	~~Climate~~	~~(Mean ± SD)~~	~~(Max to Min)~~	~~N~~	~~(Mean ± SD)~~	~~(Max to Min)~~	~~N~~
~~SP008~~	~~Spain~~	~~Mediterranean~~	~~2216 ± 878~~	~~3438 968~~	~~5~~	~~1079 ± 956~~	~~1755 403~~	~~2~~
~~SP014~~	~~Spain~~	~~Mediterranean~~	~~2364 ± 1145~~	~~3779 663~~	~~7~~	~~542 ± 205~~	~~811 238~~	~~7~~
~~SP019~~	~~Spain~~	~~Mediterranean~~	~~1573 ± 757~~	~~2903 376~~	~~9~~	~~469 ± 506~~	~~1560 338~~	~~9~~
~~SP026~~	~~Spain~~	~~Mediterranean~~	~~190 ± 383~~	~~538 454~~	~~6~~	~~346 ± 190~~	~~603 98~~	~~6~~
~~SP028~~	~~Spain~~	~~Mediterranean~~	~~6289 ± 2693~~	~~9765 2160~~	~~6~~	~~259 ± 442~~	~~817 234~~	~~4~~
~~SP029~~	~~Spain~~	~~Mediterranean~~	~~3071 ± 1919~~	~~6308 1501~~	~~5~~	~~741 ± 304~~	~~1147 435~~	~~5~~
~~SP030~~	~~Spain~~	~~Mediterranean~~	~~5356 ± 2111~~	~~7873 2692~~	~~6~~	~~198 ± 108~~	~~338 62~~	~~6~~
~~SP032~~	~~Spain~~	~~Mediterranean~~	~~2503 ± 973~~	~~4126 761~~	~~9~~	~~405 ± 283~~	~~890 25~~	~~9~~
~~SP035~~	~~Spain~~	~~Mediterranean~~	~~2133 ± 1088~~	~~3224 395~~	~~5~~	~~489 ± 504~~	~~1211 40~~	~~4~~
~~SP040~~	~~Spain~~	~~Mediterranean~~	~~3815 ± 3116~~	~~6200 289~~	~~3~~	~~–~~	~~–~~	~~0~~
~~SP041~~	~~Spain~~	~~Mediterranean~~	~~295 ± 148~~	~~421 100~~	~~4~~	~~–~~	~~–~~	~~0~~

SP043	Spain	Mediterranean	684 ± 899	1991 20	4	–	–	0
SP044	Spain	Mediterranean	46 ± 221	359 256	5	558 ± 291	991 228	6
SP045	Spain	Mediterranean	452 ± 598	1109 611	6	–	–	0
SP046	Spain	Mediterranean	487 ± 342	988 235	4	396 ± 220	616 127	5
SP049	Spain	Mediterranean	242 ± 280	798 24	6	243 ± 179	471 62	5
BE059	Belgium	Temperate	–	–	0	1726 ± 1762	4308 347	4
BE065	Belgium	Temperate	–	–	0	725 ± 224	937 414	4
DE001	Germany	Temperate	–	–	0	491 ± 248	785 147	6
DE007	Germany	Temperate	1079 ± 680	2143 459	7	–	–	0
DE011	Germany	Temperate	4889 ± 1085	6378 3866	4	–	–	0
DE012	Germany	Temperate	1391 ± 305	1677 857	6	–	–	0
DE016	Germany	Temperate	–	–	0	452 ± 468	718 381	5
DE019	Germany	Temperate	2333 ± 576	2814 1424	5	1534 ± 490	2108 1113	5
DE028	Germany	Temperate	1669 ± 634	2291 696	6	365 ± 530	1252 99	5
DE030	Germany	Temperate	1831 ± 309	2156 1490	4	136 ± 104	277 26	6
DE031	Germany	Temperate	–	–	0	1666 ± 332	2182 1268	5
DK018	Denmark	Temperate	3656 ± 3755	9657 55	6	353 ± 51	389 317	2
DK034	Denmark	Temperate	–	–	0	440 ± 281	868 201	5
DK042	Denmark	Temperate	–	–	0	127 ± 269	634 148	6

The studied ponds exhibited significant climatic and seasonal variability in their hydro-geomorphological and sediment characteristics (Table A2~~1~~, S2~~1~~). Mediterranean ponds exhibited higher air and sediment temperatures~~, shorter hydroperiods,~~ typically drying in summer. . They also showed lower sediment water content and reduced macrophyte coverage ~~consistent with an earlier drying period~~ (Table S2~~1~~). In contrast, Temperate ponds exhibited lower air and sediment temperatures, higher sediment water content, and greater macrophyte coverage ~~In contrast, Temperate ponds had lower temperatures, longer hydroperiods and in some cases, a delayed onset of drying into autumn. These ponds also displayed higher sediment water content and macrophyte coverage (~~(Table S2~~1~~). Seasonal variation was significant only for sediment temperature (U = 0, n_1 = 23, n_2 =23, p < .001, r = .86). Regarding sediment characteristics, PARAFAC analysis of fluorescent DOC yielded a three-component ~~model.~~model. The components were expressed ~~expressed~~ as the percentage contribution of each component to the total fluorescent DOC. We identified the main components as: component 1 (C1), corresponding to terrestrial humic-like substances, component 2 (C2), corresponding to humic-like substances, and component 3 (C3), corresponding to tryptophan-like substances (Table S3–S5~~; Fig. S7~~). Considering sediment composition, Mediterranean ponds exhibited lower organic matter and DOC but higher content of C2 (humic-like) compared to Temperate ponds (Table S2). Consistent with we~~t~~t -phase physicochemical patterns, Mediterranean ponds showed lower concentrations of TN, TP, and chlorophyll a than Temperate ponds. Temperate ponds also had a higher percentage of pasture within 5 m and 100 m buffer zones~~,~~ and a larger proportion of urban area within the 100 m buffer (Table S2).~~Considering sediment composition, Mediterranean ponds exhibited lower organic matter and DOC but a higher content of C2 (humic-like), whereas Temperate ponds showed higher organic matter and DOC with a comparatively lower proportion C2 content (Table S1).~~

3.1 Climate, season, and hydroperiod variation in CO_2 emissions

CO_2 emissions from the Mediterranean ponds ranged from 242 to 3877 mg C m^{-2} d^{-1} (mean ± SD: 1394 ± 1207, median = 1212, N~~n~~ = 16), while emissions from Temperate ponds ranged from 127 to 4889 mg C m^{-2} d^{-1} (mean ± SD: 1403 ± 1239, median = 1078, N~~n~~ = 14). Fluxes did not differ between climate regions (U = 104, n_1 = 16, n_2 =14, p = .76, r = .06; Fig. 3). However, we found significant seasonal differences in fluxes (U = 119, n_1 = 23, n_2 =23, p =.001, r = .47; Fig. 3). During summer, fluxes ranged from 46 to 6289 mg C m^{-2} d^{-1} (mean ± SD: 2111 ± 1739, median: 1831, N~~n~~ = 23), whereas in autumn,
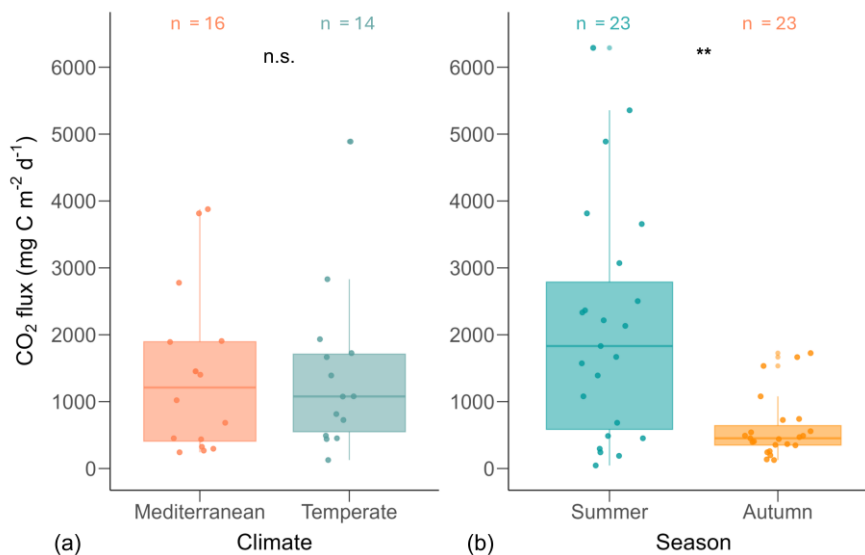
fluxes were significantly lower, ranging from 127 to 1726 mg C m^{-2} d^{-1} (mean ± SD: 598 ± 464, median: 452, ~~N~~ ~~n~~= 23).

Figure 3. Boxplots of CO₂ fluxes by climate (a) and season (b). Each point represents the mean CO₂ flux per pond, calculated from multiple replicate measurements. Asterisks (**) indicate statistically significant differences based on Mann–Whitney U tests (p < .01); n.s. denotes non-significant differences. The number of ponds (n) is indicated above each boxplot. Boxplot structure is described in Figure 2 ~~indicate statistically significant differences based on ANOVA (p<0.001); NS denotes non-significant differences. The number of ponds (n) is indicated above each boxplot. Boxplot structure is described in Figure 2~~.

365

The linear mixed-effects model (LMM) assessing the influence of hydroperiod length across season and climate regions on CO₂ fluxes revealed a significant three-way interaction among season, climate and hydroperiod (R^2_m = .33, R^2_c = .58, $p <$ .01). This indicates that the effect of hydroperiod was season-specific and climate-dependent (Fig. 4). Specifically, hydroperiod length significantly influenced CO₂ emissions only during summer in both climate regions ($p <$ .001). In Mediterranean ponds, longer hydroperiods were associated with increased CO₂ emissions ($p <$ .001), whereas in Temperate ponds, the trend was inverse but not statistically significant ($p <$ .13) (Table 1~~3~~).

370

375

Figure 4. Relationship between CO₂ fluxes and hydroperiod length (months) by climate~~s~~ and season~~s~~. Points represent individual ponds. Solid lines show linear regressions by season (blue = summer; orange = autumn) with 95% confidence intervals shaded. Marginal and conditional R² values and p-value are shown within the plot.~~The dashed line represents the overall trend.~~
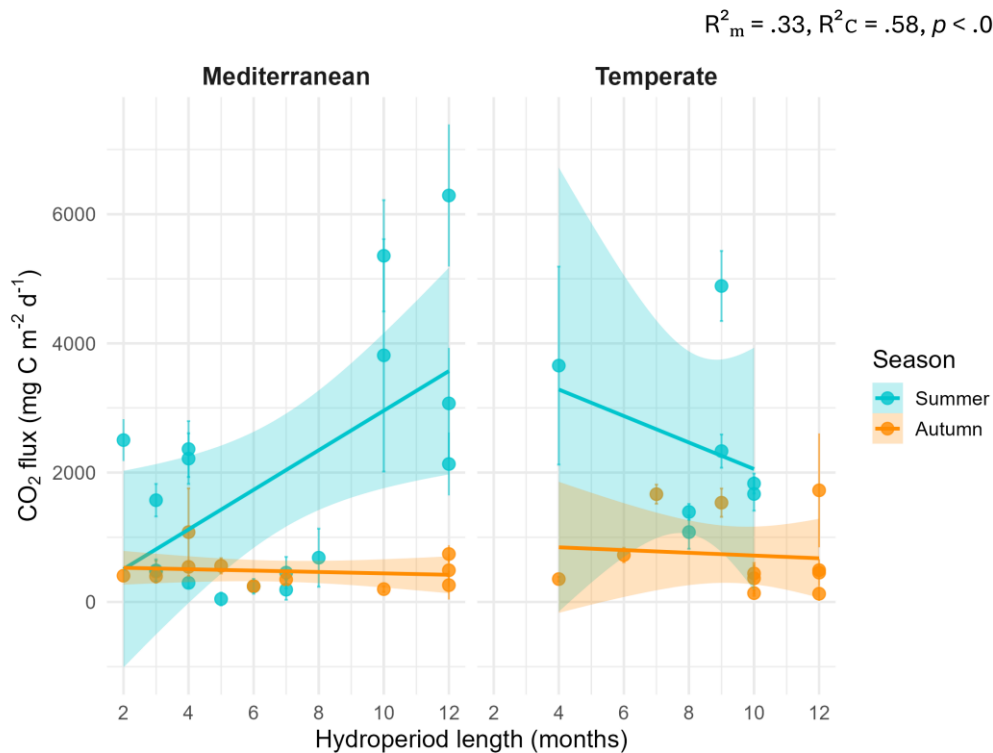
Table 13. Estimated slopes (effects) of hydroperiod length on CO_2 ~~emissions~~fluxes for each combination of season (summer and autumn) and climate region (Mediterranean and Temperate). Values are derived from the linear model assessing the interaction between hydroperiod, season, and climate. Abbreviations: SE = standard error; df = degrees of freedom; CL = confidence limit; CI = confidence interval.

Climate	Season	Estimate	SE	df	lower.CL	upper.CL	p-value
Mediterranean	Summer	290.82	78.69	27.80	129.58	452.06	<0.001
Mediterranean	Autumn	17.98	81.67	31.40	-148.49	184.46	0.83
Temperate	Summer	-264.01	172.97	68.92	-609.09	81.08	0.13
Temperate	Autumn	-17.04	131.82	38.03	-283.89	249.81	0.90

We also explored the relationship between CO_2 fluxes and temperature (annual and 40-year mean), a variable that displayed a moderately strong inverse correlation with hydroperiod length (Fig. B1). Despite this correlation, the overall regression model encompassing emissions from all ponds, and the regressions conducted for each climate region, did not yield a significant relationship ($p > .05$).

3.2 Drivers of CO_2 ~~emissions~~fluxes

The variables identified as potential predictors of CO_2 fluxes were sediment water content, sediment temperature, hydroperiod length, conservation status, macrophyte coverage, PVI, pH, maximum depth, conductivity, carbonate content, DOC, BIX, HIX, and SUVA, which exhibited correlation coefficients (r) predominantly between 0.6 and -0.6 (Fig. B1; B2). The remaining variables were excluded due to high collinearity ($|r| > 0.6$) or lack of significant association with CO_2 fluxes during the dry phase, in the case of land-use and water physicochemical variables. ~~Land use variables and water physicochemical variables were excluded from the final analysis due to their lack of significant association with CO_2 emissions during the dry phase~~. Although DOC components (C1, C2, C3) were excluded from the analysis because of their strong correlation with fluorescence indices (FI, HIX, and BIX), they provide complementary insights into DOC transformation and degradation patterns, presented in the supplementary material (Figs. S2–S5). ~~We excluded absorbances at 254 and 300, FI, air temperatures (40-year and annual means), precipitation (40-year and annual means), organic matter content and components (C1, C2, C3), due to their high collinearity ($|r| > 0.6$). Organic matter content exhibited a moderately strong and positive correlation with the macrophyte coverage and strong positive with DOC. Fluorescence indexes and components showed strong correlations. HIX positively correlated with terrestrial humic-like (C1) and humic-like (C2) components, and negatively with Tryptophan-like (C3) and BIX. This indicates that when organic matter is highly humified, stable, and refractory (high HIX and values), fresh, labile components, such as tryptophan-like or indicated by high BIX index, are low. Additionally, a strong negative correlation between FI and C1 suggest that higher contributions of terrestrial organic matter correspond to lower FI values, reflecting a dominant allochthonous source. Further details on organic matter components, are provided in the supplementary material (Figs. S2–S5). Land use variables and water physicochemical variables were excluded from the final analysis due to their lack of significant association with CO_2 emissions during the dry phase.~~

The GLMM analysis revealed significant effects of sediment water content, sediment temperature, pond conservation status, carbonate content and the interaction between sediment temperature and water content (Table 24). The model only including the interaction between sediment temperature and water content, had a marginal R^2 of 0.35, highlighting the importance of these factors in explaining CO_2 fluxes. Additionally, incorporating the second-degree polynomial improved our model by lowering the AIC and increasing the marginal R^2 to 0.38, thereby better capturing the curvilinear relationship between water content and temperature (Fig. 5). At lower temperatures (e.g., ~9.4 °C), CO_2 emissions increased slightly with sediment water content up to approximately 44%, beyond which the fluxes declined. At intermediate temperatures (~18.2 °C), sediment water content had a moderate effect ~~in~~ on CO_2 fluxes. In contrast, at higher temperatures (~27.7 °C), the trend reversed, and greater sediment water content ~~leading~~ led to increased CO_2 emissions. However, beyond ~50% water content, this effect could not be reliably assessed: confidence intervals widened substantially, reflecting the lack of observed data in this range and the consequent extrapolation of model predictions (Fig. 5). Finally, the CO_2 fluxes showed a positive relationship with conservation status and a negative relationship with carbonate content (Table 35).

Table 24. Model comparison of generalized linear mixed models (GLMMs) explaining CO_2 ~~fluxes~~emissions during the dry phase in ponds. The best model, selected based on AIC (Akaike Information Criterion), is highlighted in bold. Abbreviations: BIC = Bayesian Information Criterion; df = degrees of freedom. Temperature refers to sediment temperature.

Model fixed effects	AIC	BIC	Deviance	Log-likelihood	Marginal R^2	Conditional R^2	N	df
None (null model)	684.92	695.47	678.92	-339.461	NA	.266	249	3
Temperature	655.71	669.78	647.71	-323.85	.123	.429	249	4
Water content x Temperature	604.55	625.65	592.55	-296.27	.3475	.515	249	6
(Water content + Water content ^{2}) x Temperature	585.996	614.14	566.997	-284.995	.3788	.525	249	8
(Water content + Water content ^{2}) x Temperature + Conservation status	583.81	615.47	565.81	-282.913	.416	.520	249	9
(Water content + Water content ^{2}) x Temperature + Carbonate content	581.27	612.9	563.27	-281.63	.392	.554	248	9
(Water content + Water content ^{2}) x Temperature + Conductivity	584.945	619.60	566.947	-283.45	.403	.545	249	9
(Water content + Water content ^{2}) x Temperature + Conservation status + Conductivity	584.65	619.82	564.64	-282.32	.431	.545	249	10
(Water content + Water content ^{2}) x Temperature + Conservation status + Carbonate content	**578.43**	**613.56**	**558.43**	**-276.15**	**.431**	**.543**	**248**	**10**
(Water content + Water content ^{2}) x Temperature + Conservation status + Carbonate content + Conductivity	578.76	617.41	556.76	-278.38	.447	.555	248	11
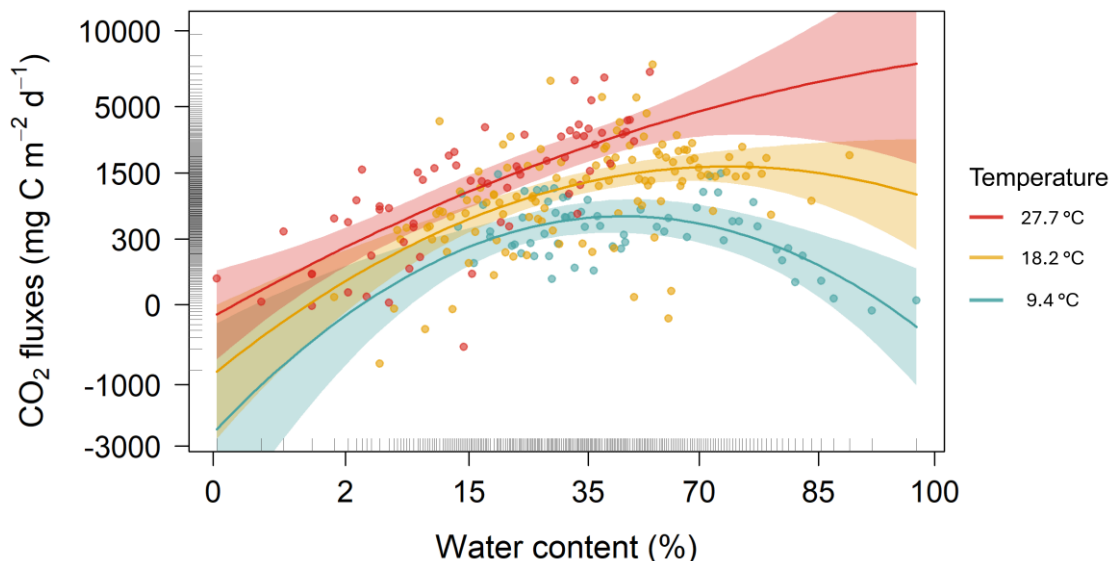
Figure 5. Partial plot effects of the interaction between sediment water content and sediment temperature on CO_2 fluxes. The figure shows results from a Generalized Linear Mixed Model (GLMM) with axes ~~back transformed~~back-transformed from ORQ (Ordered Quantile normalization) to the original scale. Each dot represents model-adjusted values, coloured lines and shaded areas depict fitted trends and 95% confidence interval~~s~~: blue = 9.4 °C, ~~yellow~~green = 18.2 °C, and red = 27.7 °C

Table 3~~5~~. Results of the best Generalized Linear Mixed Model (GLMM) explaining CO_2 fluxes during the dry phase of the studied ponds. The ,Model: (Water content + Water content²) × Temperature + Conservation status + Carbonate content (random intercept for Pond). The table shows predictors, parameter estimates, 95% confidence intervals (CI), and p-values.

	CO₂ fluxes~~emissions~~		
Predictors	*Estimates*	*CI*	*p-value*
(Intercept)	0.07	-0.10 – 0.24	.407
Water content [Linear]	8.32	5.54 – 11.10	**< .001**
Water content ² [Quadratic]	-4.30	-6.90 – -1.70	**.001**
Temperature	0.54	0.41 – 0.66	**< .001**
Conservation status	0.25	0.09 – 0.42	**.003**
Carbonate content	-0.20	-0.33 – -0.08	**.002**
Water content [Linear] x Temperature	2.69	0.33 – 5.04	**.025**

Water content ^{2} [Quadratic] x Temperature	2.12	0.47 – 3.76	**.012**

Random Effects	
σ^2	0.49
$\tau_{00\ \text{Pond}}$	0.12
ICC	0.20
N_{Pond}	30
Observations	248
Marginal R^2 / Conditional R^2	.431 / .543

4 Discussion

Our study demonstrated that, overall, ponds emitted CO_2 during the dry phase, despite occasional negative fluxes observed at a few points within some ponds. Flux rates were approximately three times higher than those reported for the wet phase of similarly -sized permanent ponds (Holgerson and Raymond 2016). Seasonality strongly influenced the magnitude of emissions, with the highest fluxes observed in summer. This seasonal effect also shaped the influence of hydroperiod, which was significant only during summer and interacted with climate, leading to higher emissions in Mediterranean ponds with extended hydroperiods. The overall pattern was largely driven by the interaction between sediment temperature and water content, which followed a curvilinear relationship with a clear an apparent threshold effect. Other local factors, such as pond conservation status and carbonate content, also played a role in modulating CO_2 fluxes. Taken together, these findings suggest that changes in temperature, precipitation, hydroperiod, and pond ecological condition, driven by climate change, land use or other human-induced alterations, can significantly affect CO_2 emissions from temporary ponds.

4.1 CO2 fluxes across ponds: influence of climate, seasonality and hydroperiod

Our study showed high variability of CO_2 fluxesemissions both among and within ponds, highlighting the importance of accounting for microhabitats in assessments. As hypothesized (Hypothesis 1), we found significant seasonal variation, emphasizing the importance of the timing of the drying period, with the highest fluxes occurring under summer conditions. However, contrary to our expectations, overall CO_2 emissions did not differ significantly between climate regions (Mediterranean vs Temperate). though aligning with the findings of Keller et al. (2020) and suggestingThis finding aligns with that -of Keller et al. (2020) and suggests that local factors may outweigh broader climatic influences. The CO_2 dry fluxes reported by Keller et al. (2020)– (mean ± SD = 3204 ± 2652 mg C m^{-2} d^{-1} or 267 ± 221 mmol m^{-2} d^{-1}, N = 27), measured exclusively during the summer, were significantly higher (t-test p = .006) than the average fluxes obtained in our study (mean ± SD = 1398 ± 1201 mg C m^{-2} d^{-1} or 117 ± 100 mmol m^{-2} d^{-1}, N = 30), which encompassed a broader seasonal

range including both summer and autumn (Table 45). In contrast, there was no significant difference when comparing only summer emissions (t-test $p = .15$). Similarly, our emission values fall within the range reported for other temporary ponds that captured different stages of the drying period (i.e., seasonal variation) (Catalán et al., 2014; ~~DelVecchia et al., 2019;~~Obrador et al., 2018) (Table 4). This finding underscores the importance of assessing CO_2 emissions throughout the entire dry period, as fluxes can vary substantially over time and between seasons.

460

Table 45. CO$_2$ emissions from ponds during dry and wet phases, including mean values and standard deviation (SD) from this study and previously published studies conducted across different climate regions, seasons, and hydrological conditions.

Study	Location	Climate	CO$_2$ emissions (mg C m^{-2} d^{-1})	SD	Season	Pond type
Our study						
Overall Ponds	Europe	Temperate, Mediterranean	1398	1201	Summer, autumn	Temporary, semi-permanent, permanent
Ponds in summer	Europe	Temperate, Mediterranean	2111	1739	Summer	Temporary, semi-permanent, permanent
Ponds in autumn	Europe	Temperate, Mediterranean	598	464	Autumn	Temporary, semi-permanent, permanent
Inundated						
Holgerson and Raymond (2016)	Global (< 0.001 km^2)	Most general climates included	422	63	Not specified	Permanent
Holgerson and Raymond (2016)	Global (0.001-0.001 km^2)	Most general climates included	255	71	Not specified	Permanent
DelVecchia et al. (2019)	USA	Subalpine	129	123	Summer	Temporary, semi-permanent, permanent
Dry						
Keller et al. (2020)	Global	Tropical, temperate, polar	3204	2652	Summer	Temporary
Catalán et al. (2014)	Spain	Mediterranean	1456	1657	Summer, autumn	Temporary
Obrador et al. (2018)	Spain	Mediterranean	1294	1247	Spring, summer, autumn	Temporary
DelVecchia et al. (2019)	USA	Subalpine	1813	321	Summer	Temporary, semi-permanent and permanent
Martinsen et al. (2019)	Sweden	Temperate	2995	2090	Summer	Not specified
Fromin et al. (2010)	France	Mediterranean	120-7200	n.d.	All seasons	Temporary
DelVecchia et al. (2021)	USA	Alpine	3978	138	Summer	Temporary, semi-permanent and permanent
DelVecchia et al. (2021)	USA	Subalpine	1714	541	Summer	Temporary, semi-permanent and permanent

This temporal variability was also reflected in the role of hydroperiod length, which showed a clear seasonal dependence
modulated by regional climate. Significant differences in emissions were observed only during summer, with contrasting
trends across climate regions. Notably, the hypothesized effect of hydroperiod (Hypothesis 2) was supported only in
Mediterranean ponds, where longer hydroperiods were associated with higher CO_2 emissions. Hydroperiod showed a
moderate positive correlation with sediment water content (r = .47; Fig. B1), suggesting that longer hydroperiods are
associated with higher sediment water content. This relationship could partially explain the effect of hydroperiod on CO_2
emissions. However, other environmental factors are likely to contribute as well. Moreover, hydroperiod length was
positively correlated with increased tryptophan-like fluorescence (C3), indicating the accumulation of less processed humic-
like (C2) and more labile organic matter in the sediments (Fig. S4). The effect of both humic-like and tryptophan-like
components on CO_2 emissions exhibited clear seasonal dependence, with significant impacts observed during summer (Fig.
S5). Hydroperiod duration influences organic matter accumulation during the wet phase, which may lead to increased CO_2
emissions as sediments become more aerobic during the dry season (Downing, 2010; Fromin et al., 2010; Jarvis et al., 2007;
Marcé et al., 2019; Obrador et al., 2018; Rulík et al., 2023). In the Mediterranean, temporary ponds are experiencing shorter
hydroperiods, becoming increasingly intermittent or disappearing altogether (Gómez-Rodríguez et al., 2010). Similarly,
ponds in the Temperate region are vulnerable to shifts from permanent to semi-permanent or temporary states (Čížková et
al., 2013; Lee et al., 2015). These transitions toward more temporary systems may have important climate-warming
implications, as exposed sediments can amplify CO_2 emissions (Marcé et al., 2019). However, these emissions are strongly
influenced by the timing of pond drying, with higher magnitudes occurring under summer conditions. Our results in the
Mediterranean region, indicate that climate-driven transitions toward shorter hydroperiods and more temporary pond
conditions may actually reduce CO_2 fluxes during the dry phase. This finding highlights the need to evaluate how shifts in
hydroperiods could impact CO_2 emissions across regions; however, a complete understanding would require integrating both
wet and dry phases.

4.2 Drivers of CO_2 fluxesemissions during the dry phase

Our study identified the key drivers explaining CO_2 emissions from dry ponds pond sediments as the interaction between
sediment temperature and water content, conservation status, and carbonate content. As hypothesized (Hypothesis 3), local
factors, particularly the temperature-water content interaction, played a crucial role in CO_2 emissions from dry sediments,
aligning with previous studies on dry flux emission (Keller et al., 2020; Marcé et al., 2019; Martinsen et al., 2019; Obrador
et al., 2018; Oertel et al., 2016). Our results revealed a non-linear interaction between sediment water content and
temperature, where water content exerts a threshold effect modulated by temperature, constraining CO_2 emissions at both
low and high extremes of these variables. Low sediment water content limits microbial activity, reducing CO_2 fluxes, while
saturated conditions restrict oxygen availability and gas diffusion, suppressing aerobic respiration (Almeida et al., 2019;
Oertel et al., 2016; Sánchez-Carrillo, 2009). This effect is temperature-dependent, as rising temperatures stimulate microbial

metabolism and respiration, directly increasing CO_2 emissions (Fromin et al., 2010; Gilbert et al., 2017). Water content also influences sediment temperature, further affecting CO_2 fluxes (Sabater et al., 2016; Sponseller, 2007). These results highlight that sediment temperature and water content are interdependent drivers of carbon fluxes, underscoring the complex interplay between abiotic and biotic factors regulating these systems (Marcé et al., 2019).

500   In our study, dry sediment temperatures varied widely, ranging from 7 to 47.5 °C (mean ± SD: 18.8 ± 7.8 °C), with significant seasonal differences. In contrast, sediment water content did not differ significantly between seasons, although it showed a broad range from 0.89% to 94.2% (mean ± SD: 34.8 ± 24%). Our analysis predicts that CO_2 emissions peak at sediment temperatures around 27.7 ºC and sediment water content levels between 27% to 44%. These results indicate that maximum CO_2 fluxes occur under ~~intermediate~~ higher sediment temperature and moderate water content conditions, likely

505 optimizing microbial metabolism. These findings align with ~~Pozzo Pirotta~~Pozzo-Pirotta et al. (2022) and Gómez-Gener et al. (2016), who reported the highest emissions at temperature ranges from 18 to 25.5 °C. Conversely, temperatures exceeding ~30 °C may promote evaporation, reduce water availability and ultimately lower respiration rates due to enzyme inhibition and physiological stress (Lellei-Kovács et al., 2011). The temperature-water content relationship explains the observed seasonal pattern, with elevated temperatures enhancing microbial activity and emissions during summer, and reduced

510 activity during autumn. This pattern can also partly explain the variation in emissions across ponds with different hydroperiod lengths. Furthermore, the absence of significant differences in CO_2 fluxes~~emissions~~ between the two climate regions may reflect the predominance of local-scale drivers, as both sediment temperature and water content conditions favourable for microbial respiration, and consequently CO_2 emissions, were present in ponds across both Mediterranean and Temperate climate regions.

515 We also found a negative relationship between CO_2 fluxes~~emissions~~ and carbonate content, suggesting that carbonate-rich sediments may reduce mineralization rates, either by limiting microbial activity or through abiotic processes such as carbonate reactions. Although biological activity is the primary source of CO_2 fluxes~~emissions~~ from dry sediments, abiotic processes, such as pedochemical and geological reactions (e.g., carbonate dissolution), may also contribute, albeit typically to a lesser extent (Rey, 2015). This relationship may arise because, in some regions, carbonaceous substrates modulate CO_2

520 levels during dry periods of low biological activity through weathering and precipitation reactions involving inorganic carbon (Roland et al., 2013; Hanken, Bjørlykke and Nielsen, 2015). This could explain the occasional negative CO_2 fluxes observed in our study (mean ± SD: - 257.6 ± 191.3 mg C m^{-2} d^{-1}), which did not differ between seasons (t-test, p = .79). These values are within the range reported in studies using closed chambers, including Keller et al. (2019) (-324 mg C m^{-2} d^{-1}), Ma et al. (2013) (-290 and -436 mg C m^{-2} d^{-1} for under-canopy and inter-plant spaces, respectively), and Koschorreck et

525 al. (2022) (-1,440 to 13,620 mg C m^{-2} d^{-1}), with a similar proportion of negative fluxes (6%). Since all our measurements were conducted in reflective chambers that excluded light, it is unlikely that these negative fluxes resulted from photosynthetic CO_2 uptake by residual phytoplankton macrophytes or cryptobiotic crusts. Instead, they likely reflect sediment physico-chemical processes associated with inorganic reactions (Ma et al., 2013; Marcé et al., 2019).

Moreover, as hypothesized (Hypothesis 4), ponds in better ecological condition, i.e., those with higher conservation status
530 values, exhibited higher CO_2 emissions during the dry phase. Well-conserved ponds tend to support higher macrophyte diversity and vegetation cover, which enhances the accumulation and stabilization of organic carbon in sediments, promoting carbon sink during wet phases (Akasaka et al., 2010; Garcia-Murillo et al., 2025; Nag et al., 2023). In our study, pond conservation status (ECELS index) was positively correlated with both macrophyte coverage and PVI ($p < .001$). In turn, macrophyte cover correlated positively with sediment organic matter and DOC $(p < .001)$. During dry phases, the exposure
535 of previously vegetated sediments to air can trigger plant senescence and increase microbial activity, leading to elevated CO_2 emissions (Catalán et al., 2014; Martinsen et al., 2019). This mechanism may help explain the counterintuitive relationship between higher conservation status and increased CO_2 emissions during the dry phase. Nonetheless, these higher emissions may be offset during the wet phase by lower emissions, driven by enhanced primary production and greater carbon burial (Page and Dalal, 2011; Morant et al., 2020; Zou et al., 2022). For example, Taylor et al. (2019) found that carbon burial rates
540 ranged between 216 and 676 mg C m^{-2} d^{-1} depending on ponds' vegetation. Sharma et al. (under revision) reported that CO_2 fluxes in wetland bare zones averaged 1555 ± 3082 mg C m^{-2} d^{-1}, with no significant differences between light and dark conditions. In contrast, fluxes in wetlands vegetated zones were much more variable, reaching 4234~~7~~ $\pm$ 5789~~93~~ mg C m^{-2} d^{-1} under dark conditions and -~~=~~1066 $\pm$ 3715~~28~~ mg C m^{-2} d^{-1} under light conditions. In line with observations by Madaschi et al. (2025), vegetated soils exhibited greater ecosystem respiration than bare soils; however, their net ecosystem exchange (NEE)
545 was negative, indicating a net CO_2 uptake driven by enhanced gross primary production (GPP). Reported NEE values were 1740 ± 324 mg C m^{-2} d^{-1} for bare soils and -912 ± 288 mg C m^{-2} d^{-1} for vegetated soils. Our CO_2 flux measurements were taken from bare sediments, excluding vegetated areas, and therefore do not reflect the influence of primary production or net ecosystem metabolism. Consequently, the overall CO_2 fluxes from these systems are probably lower than those reported here.~~It is important to note that our CO_2 flux measurements were taken from bare sediment and do not account for the effects~~
550 ~~of primary production and net ecosystem metabolism, suggesting that the overall fluxes from these systems are likely lower than indicated here.~~ Finally, conservation status, represented by the ECELS index, which integrates pond morphology, human impacts, vegetation abundance, and water quality, appears to be a stronger predictor of CO_2 emissions during the dry phase than individual factors such as land use or trophic status proxies (e.g., chlorophyll a, TN, TP). This highlights the value of integrative ecological indices over isolated proxies when evaluating pond function.

555 **4.3 Implications of our study in the context of global change**

Overall, our results emphasize the importance of assessing CO_2 emissions throughout the entire dry period, as key drivers such as sediment temperature and water content can fluctuate over short time scales and are strongly influenced by climatic conditions. Capturing this temporal variability is critical, as single-time-point measurements may underestimate the actual emissions dynamics of these ecosystems. Incorporating this variability into carbon budgets will improve their accuracy and
560 enhance the design of climate mitigation strategies that consider CO_2 emissions from dry sediments. Despite their relevance,

studies quantifying CO_2 fluxes during dry phases remain scarce, creating a critical knowledge gap that limits the inclusion of temporary systems into global GHG inventories (Keller et al., 2020; Lauerwald et al., 2023; Marcé et al., 2019).

Our findings also suggest that projected increases in temperature are likely to elevate sediment temperatures, which, especially when combined with episodic rewetting events, may substantially enhance CO_2 emissions during dry phases. In addition, ponds with longer ~~more permanent~~ hydroperiods exhibited higher dry-phase CO_2 fluxes than ephemeral systems in Mediterranean regions. However, to fully understand how shifts in hydroperiod toward increased intermittency affect carbon dynamics, future studies should integrate measurements from both wet and dry phases.

Understanding these processes is essential in the context of climate change, as climate regions are facing divergent hydrologic trends (Pekel et al., 2016; Wang et al., 2018; Vicente-Serrano et al., 2022; Bevacqua et al., 2024). Given that extreme events, such as the severe 2022 European drought (Copernicus Climate Change Service (C3S), 2023), are expected to become more frequent, and that anthropogenic pressures continue to intensify, inland water systems are undergoing rapid transformations that will increasingly influence the global carbon cycle.

Conclusion

Our results highlight the need to integrate CO_2 emissions across all stages of the dry season to achieve accurate estimates of fluxes in ponds. Although no significant differences in emissions were observed among climatic regions, key drivers such as hydroperiod length, sediment temperature, and sediment water content are inherently linked to climate. Moreover, ponds with better conservation status emitted more CO_2 during the dry phase; however, a comprehensive integration with fluxes from the wet phase is still required. Understanding these dynamics is crucial for predicting carbon fluxes in pond ecosystems under future climate and land-use scenarios.

Appendix A: Pond sampling, hydro-geomorphological and sediment characteristics

Table A1. Geographic location and sampling details of the studied ponds, including pond identifiers, pondscape name, hydrological classification, coordinates (longitude and latitude), and sampling dates and times during summer and autumn campaigns.

Pond ID	Pond Code	Country	Pondscape	Hydrological classification	Longitude	Latitude	Date Summer	Time summer start	Time summer finish	Date Autumn	Time autumn starts	Time autumn finish
SP008	ALB_5	Spain	Albera	Temporary	2.980	42.397	6/7/2022	13:47:00	14:47:00	14/11/2022	15:17:00	16:17:00
SP014	ALB_3	Spain	Albera	Temporary	2.959	42.379	6/7/2022	11:37:00	12:37:00	14/11/2022	12:40:00	13:50:00
SP019	ALB_4	Spain	Albera	Temporary	2.983	42.382	6/7/2022	16:16:00	17:31:00	14/11/2022	10:00:00	11:20:00
SP026	OSO_1	Spain	Osona	Temporary	2.352	41.961	7/7/2022	08:07:00	09:08:00	15/11/2022	09:42:00	10:42:00
SP028	OSO_3	Spain	Osona	Semi-permanent	2.363	41.964	7/7/2022	09:46:00	10:46:00	15/11/2022	16:02:00	16:37:00
SP029	OSO_4	Spain	Osona	Semi-permanent	2.374	41.968	7/7/2022	14:29:00	15:29:00	15/11/2022	11:52:00	12:52:00
SP030	OSO_5	Spain	Osona	Temporary	2.375	41.963	7/7/2022	13:07:00	14:07:00	15/11/2022	13:36:00	14:31:00
SP032	SEL_1	Spain	Selva	Temporary	2.718	41.829	4/7/2022	11:26:00	13:06:00	24/11/2022	09:42:00	11:20:00
SP035	SEL_4	Spain	Selva	Temporary	2.725	41.819	4/7/2022	14:54:00	15:54:00	24/11/2022	12:31:00	13:10:00
SP040	GAR_3	Spain	Garrtoxa	Semi-permanent	2.501	42.284	13/7/2022	12:15:00	13:15:00	-	-	-
SP041	GAR_4	Spain	Garrtoxa	Temporary	2.498	42.289	13/7/2022	09:33:00	10:33:00	-	-	-
SP043	GAR_6	Spain	Garrtoxa	Temporary	2.556	42.268	13/7/2022	15:25:00	16:13:00	-	-	-
SP044	GAV_1	Spain	Gavarres	Temporary	2.922	41.836	5/7/2022	16:09:00	17:09:00	16/11/2022	15:10:00	14:10:00
SP045	GAV_2	Spain	Gavarres	Semi-permanent	2.878	41.842	12/7/2022	10:55:00	11:55:00	-	-	-
SP046	GAV_3	Spain	Gavarres	Temporary	2.895	41.870	5/7/2022	11:34:00	12:34:00	23/11/2022	09:53:00	10:53:00
SP049	GAV_6	Spain	Gavarres	Temporary	2.895	41.865	12/7/2022	12:50:00	13:50:00	23/11/2022	11:40:00	12:40:00
BE059	FB1_EX2	Belgium	Flemish_Brabant	Permanent	4.943	50.929	-	-	-	5/10/2022	18:49:00	19:36:26
BE065	LB2_IN2	Belgium	Bocholt	Temporary	5.605	51.195	-	-	-	5/10/2022	15:00:00	15:45:00
DE001	MUN_56	Germany	Muncheberg	Permanent	14.112	52.474	-	-	-	29/9/2022	12:43:00	14:12:00
DE007	SCH_07	Germany	Schoneiche	Temporary	13.699	52.481	11/7/2022	13:46:00	17:05:00	-	-	-
DE011	LIE_12	Germany	Lietzen	Temporary	14.353	52.459	12/8/2022	11:30:00	12:33:00	-	-	-
DE012	LIE_09	Germany	Lietzen	Temporary	14.353	52.460	15/7/2022	12:09:00	16:05:00	-	-	-
DE016	QUI_ex5	Germany	Quillow	Semi-permanent	13.623	53.322	28/9/2022	14:08:00	15:07:00	-	-	-
DE019	QUI_ex2	Germany	Quillow	Temporary	13.567	53.307	14/7/2022	10:34:00	11:38:00	5/10/2022	09:10:00	11:00:00
DE028	MUN_41	Germany	Muncheberg	Semi-permanent	14.145	52.472	5/8/2022	13:24:00	17:09:00	6/10/2022	11:04:00	12:30:00
DE030	MUN_105	Germany	Muncheberg	Temporary	14.145	52.522	12/7/2022	14:54:00	16:20:00	30/9/2022	11:06:00	13:13:00
DE031	MUN_201	Germany	Muncheberg	Temporary	14.133	52.530	-	-	-	30/9/2022	14:58:00	15:09:00
DK018	PAE6	Denmark	Aero	Temporary	10.319	54.902	11/7/2022	11:39:15	12:41:46	15/11/2022	11:53:45	12:01:15
DK042	PAE2	Denmark	Aero	Permanent	10.348	54.866	-	-	-	14/11/2022	11:06:00	11:58:00
DK034	PAE4	Denmark	Aero	Semi-permanent	10.329	54.874	-	-	-	15/11/2022	07:56:00	09:41:02

585   Table A2. Hydro-geomorphological and sediment characteristics of the studied ponds.

Pond	Country	Climate	Area (m²)	Maximum depth (cm)	Hydroperiod length (mMonths)	Season	Temperature (°C)	Water content (%)	pH	Conductivity (μS/cm⁻¹)	Carbonate content (%)	Organic matter (%)	DOC (mg C/g⁻¹)
SP008	Spain	Mediterranean	2555.36	127	4	Summer	24.94	12.80	4.99	314.6	0.73	16.01	2.36
						Autumn	18.2	19.51	4.93	420.4	1.25	12.52	1.17
SP014	Spain	Mediterranean	13465.72	121	4	Summer	22.27	29.87	4.91	595.71	1.44	23.69	1.18
						Autumn	16.44	19.07	4.77	786	1.76	23.77	1.77
SP019	Spain	Mediterranean	11455.29	125	3	Summer	25.4	19.40	5.08	389.22	0.94	17.08	1.66
						Autumn	14.66	14.32	5.05	456.22	1.34	17.68	1.52
SP026	Spain	Mediterranean	176.62	77	7	Summer	20.15	3.59	7.53	957.5	0.15	2.78	0.39
						Autumn	10.43	27.95	7.47	459.67	22.53	4.33	0.4
SP028	Spain	Mediterranean	324.84	104	12	Summer	18.83	32.39	7.2	718.17	0.22	5.85	0.48
						Autumn	12.25	41.30	7.2	318	19.72	8.74	0.62
SP029	Spain	Mediterranean	128.52	140	12	Summer	26.74	39.30	7.24	422.6	3.52	16.78	0.56
						Autumn	10.98	30.93	7.38	334.8	18.95	5.21	0.48
SP030	Spain	Mediterranean	248.35	137	10	Summer	25.83	38.78	7.22	556.33	0.21	5.39	0.74
						Autumn	11.42	38.39	7.26	325.83	18.39	5.7	0.56
SP032	Spain	Mediterranean	565.29	146	2	Summer	25.98	31.87	7.3	713.22	0.52	6.23	0.38
						Autumn	9.29	24.47	7.52	336.22	1.46	6.26	0.47
SP035	Spain	Mediterranean	307.70	118	12	Summer	27.82	38.32	6.97	244.34	0.1	6.17	0.63
						Autumn	12.68	29.42	6.84	134.88	0.69	4.4	0.5
SP040	Spain	Mediterranean	86.05	85	10	Summer	26.98	43.65	7.39	480.25	20.91	7.15	1.32
SP041	Spain	Mediterranean	84.39	72	4	Summer	27.36	2.51	7.76	282.8	5.31	10.37	1.47
SP043	Spain	Mediterranean	157.48	58	8	Summer	39.33	2.15	7.67	462.5	21.84	14.33	1.92
SP044	Spain	Mediterranean	1205.68	93	5	Summer	33.17	3.63	7.39	628.33	0.89	11.71	0.83
						Autumn	15.03	33.91	7.84	245.83	8.52	12.37	1.23
SP045	Spain	Mediterranean	65.42	148	7	Summer	26.77	13.49	6.38	131.33	0.44	1.78	0.33
SP046	Spain	Mediterranean	504.42	72	3	Summer	32.76	5.02	5.61	106.64	0.13	15.28	4.6
						Autumn	8.56	20.16	5.61	106.64	0.8	3.99	0.63
SP049	Spain	Mediterranean	99.40	73	6	Summer	32	3.97	6.11	147.22	1.3	7.69	0.46
						Autumn	9.08	20.56	5.87	96.52	0.83	2.27	0.29
BE059	Belgium	Temperate	98	87	12	Autumn	16.33	21.04	6.11	485.53	0.73	5.08	0.64
BE065	Belgium	Temperate	380	83.75	6	Autumn	16.55	9.31	6.17	59.83	0.33	1.15	0.3
DE001	Germany	Temperate	2250	262	12	Autumn	12.3	80.96	7.25	453.67	1.54	46.89	7.67
DE007	Germany	Temperate	1350	170	8	Summer	19.99	63.59	6.73	305.33	1.08	32.2	2.04
DE011	Germany	Temperate	1500	83	9	Summer	21.5	66.37	7.35	457.83	14.8	20.75	2.33
DE012	Germany	Temperate	2800	69	8	Summer	19.95	68.92	7.57	1484.5	13.41	21.93	2.15
DE016	Germany	Temperate	150	160	12	Autumn	13.8	61.11	6.96	462.2	2.12	11.32	1.8
DE019	Germany	Temperate	60	70	9	Summer	19.7	41.15	5.61	615	2.28	12.53	1.28
DE028	Germany	Temperate	600	115	10	Summer	24.64	23.06	6.65	741	1.59	8.16	0.79
						Autumn	13.52	19.46	6.29	1504.8	1.39	7.26	1.52
DE030	Germany	Temperate	1200	55	10	Summer	23.81	75.01	7.12	581.2	2.04	33.58	1.89
						Autumn	10.83	79.48	6.77	450.83	3.7	39.69	2.84
DE031	Germany	Temperate	800	45	7	Autumn	11.89	76.53	7.18	1087.6	5.07	69.51	4.04
DK018	Denmark	Temperate	820	78	4	Summer	20.48	51.13	6.75	302.83	1.08	13.27	1.5
						Autumn	8.9	55.58	6.88	107.6	1.02	12.73	1.44
DK034	Denmark	Temperate	190	103	10	Autumn	7.7	71.39	7.54	507.02	21.39	14.59	3.48
DK042	Denmark	Temperate	645	100	12	Autumn	9.42	80.25	6.54	529.99	1.87	29.63	9.48

Table A3. List of variables measured in this study, grouped by spatial scale: regional, landscape, local, sediment and water characteristics, dissolved organic matter and components of organic matter based on PARAFAC (Parallel Factor Analysis).

	Variable	Type	Unit
Regional	Temperature 40-year average (1978-2018)	Continuous	K
	Precipitation 40-year average (1978-2018)	Continuous	mm m^{-1}
	Climate	Categorical	(Mediterranean, Temperate)
	Annual temperature (2022)	Continuous	°C
	Annual precipitation (2022)	Continuous	mm
	Latitude	Continuous	Decimal degrees (WGS 84)
Landscape	Open nature (5 m and 100)	Continuous	%
	Forest (5 m and 100)	Continuous	%
	Pasture (5 m and 100)	Continuous	%
	Arable (5 m and 100)	Continuous	%
	Grassland (5 m and 100)	Continuous	%
	Urban (5 m and 100)	Continuous	%
Local pond characteristics	ECELS index (Conservation status)	Continuous	0-100
	Coverage	Continuous	%
	PVI (plant volume inhabited)	Continuous	%
	Hydroperiod length	Continuous	months
	Area	Continuous	m^2
	Maximum depth	Continuous	cm
Water characteristics	Chlorophyll a	Continuous	µg L^{-1}
	Total Nitrogen	Continuous	mg L^{-1}
	Total phosphorus	Continuous	mg L^{-1}
	Dissolved organic carbon (DOC)	Continuous	mg L^{-1}
Sediment characteristics	Temperature	Continuous	°C
	Water content	Continuous	%
	Organic matter	Continuous	%
	Carbonate content	Continuous	%
	pH	Continuous	-
	Conductivity	Continuous	µS cm^{-1}
	Texture	Categories	(Clay, Sandy, Loamy)
Dissolved organic matter	Dissolved organic carbon (DOC)	Continuous	mg C g^{-1}
	Absorbance at 254 nm (Abs254)	Continuous	-
	Absorbance at 300 nm (Abs300)	Continuous	-
	BIX (biological index)	Continuous	-
	HIX (Humification index)	Continuous	-
	FI (fluorescence index)	Continuous	-
	SUVA (Specific Ultraviolet Absorbance)	Continuous	L mg C^{-1} m^{-1}
PARAFAC	C1 Terrestrial humic-like	Continuous	-
	C2 Humic-like	Continuous	-
	C3 Tryptophan-like	Continuous	-

Appendix B: Ceorrelation among variables

Figure B1. Correlation matrix of environmental and sediment variables assessed in relation to CO_2 fluxesemissions in ponds. Pearson correlation coefficients (R) are displayed within the cells. The colour scale represents the strength and direction of the correlations, with red indicating positive and blue indicating negative relationships. Abbrev. C1 = terrestrial humic-like, C2 = humic-like and C3 = tryptophan-like.
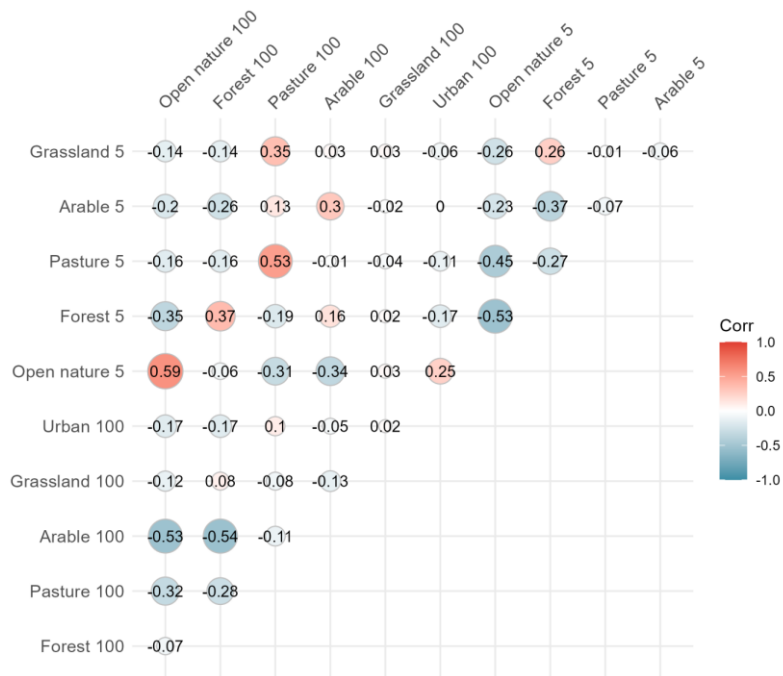
Figure B2. Correlation matrix of land use variables at 5m and 100m scales assessed in relation to CO_2 ~~fluxes~~emissions in ponds. Pearson correlation coefficients (R) are shown within the matrix. The colour scale represents correlation strength and direction, with red indicating positive and blue indicating negative relationships.

Data availability

The datasets used in this study will be available upon reasonable request.

Author contribution

CT and SB conceived the study and helped supervise the project; VFA and CT developed the theory and performed the computations; VFA, LMP, CT, SB, PL, TB, and TD collected the field data; VFA, CT and LMP performed the laboratory analyses; RM supported the sediment analyses and provided material and infrastructure; TB and TD designed the CO_2 sensors and scripts for gas data collection; VFA analysed the data with support from CT, TB, and RM; VFA wrote the manuscript with substantial input from CT and SB; all authors revised, edited and approved the final version of the manuscript.

Competing interests

The contact author has declared that none of the authors has any competing interests.

Acknowledgements

We thank the PONDERFUL consortium; especially the staff of Aquatic Ecology Group (GEA) of the University of Vic - Central University of Catalonia, the GRECO research teams of the Institute of Aquatic Ecology of the University of Girona, the Aarhus University (AU), and the Leibniz-Institute of Freshwater Ecology and Inland Fisheries (IGB), for assistance in the field and technical assistance. The authors acknowledge the use of the AI language model ChatGPT (OpenAI) to assist in improving the English language and writing style of this manuscript.

Financial support

This research has received funding from the European Union's research and innovation programme (H2020) under grant agreement No 869296 – The PONDERFUL Project. SB, TAD, TB, and CT have also received funding from the MCIN/AEI/10.13039/501100011033/UE under the Biodiversa + TRANSPONDER grant (PCI2023-145983-2). VFA has a PhD fellowship from AGAUR-FI predoctoral program (2024 FI-3 00755) Joan Oró of the Secretariat of Universities, and Research of the Department of Research, and Universities of the Generalitat de Catalunya and the European Social Fund Plus. CT is a CONICET (Argentinean Council of Science) researcher. RM participated through the project Alter-C (Spanish Agencia Estatal de Investigación grant PID2020-114024GB-C32/AEI/10.13039/501100011033).

References

Agnew, D., Fryirs, K. A., Ralph, T. J., and Kobayashi, T.: Soil carbon dynamics and aquatic metabolism of a wet–dry tropics wetland system, Wetl Ecol Manag, 29, 1–25, https://doi.org/10.1007/s11273-020-09745-w, 2021.

Akaike, H.: Information Theory and an Extension of the Maximum Likelihood Principle, in: Selected Papers of Hirotugu Akaike, edited by: Parzen Emanuel and Tanabe, K. and K. G., Springer New York, New York, NY, 199–213, https://doi.org/10.1007/978-1-4612-1694-0_15, 1998.

Akasaka, M., Takamura, N., Mitsuhashi, H., and Kadono, Y.: Effects of land use on aquatic macrophyte diversity and water quality of ponds, Freshw Biol, 55, 909–922, https://doi.org/10.1111/j.1365-2427.2009.02334.x, 2010.

Almeida, R., Paranaíba, J., Barbosa Alves, Í., Sobek, S., Kosten, S., Linkhorst, A., Mendonça, R., Quadra, G., Roland, F., and Barros, N.: Carbon dioxide emission from drawdown areas of a Brazilian reservoir is linked to surrounding land cover, Aquat Sci, 81, 68, https://doi.org/10.1007/s00027-019-0665-9, 2019.

Baastrup-Spohr, L., Møller, C. L., and Sand-Jensen, K.: Water-level fluctuations affect sediment properties, carbon flux and growth of the isoetid Littorella uniflora in oligotrophic lakes, Freshw Biol, 61, 301–315, https://doi.org/10.1111/fwb.12704, 2016.

640 Bartoń, K.: MuMIn: Multi-Model Inference, R package version 1.48.11, CRAN, 10.32614/CRAN.package.MuMIn, 2023.

Bartrons, M., Yang, J., Cuenca Cambronero, M., Lemmens, P., Anton-Pardo, M., Beklioğlu, M., Biggs, J., Boissezon, A., Boix, D., Calvo, C., Colina, M., Davidson, T. A., De Meester, L., Fahy, J. C., Greaves, H. M., Kiran Isufi, H., Levi, E. E., Meerhoff, M., Mehner, T., Mülayim, E. B., Oertli, B., Patmore, I. R., Sayer, C. D., Villà-Freixa, J., and Brucet, S.: Why ponds concentrate nutrients: the roles of internal features, land use, and climate, Hydrobiologia, 645 https://doi.org/10.1007/s10750-025-05907-0, 2025.

Bates, D., Mächler, M., Bolker, B., and Walker, S.: Fitting Linear Mixed-Effects Models Using lme4, J Stat Softw, 67, 1–48, https://doi.org/10.18637/jss.v067.i01, 2015.

Bastviken, D., Sundgren, I., Natchimuthu, S., Reyier, H., and Gälfalk, M.: Technical Note: Cost-efficient approaches to measure carbon dioxide (CO_2) fluxes and concentrations in terrestrial and aquatic environments using mini loggers, 650 Biogeosciences, 12, 3849–3859, https://doi.org/10.5194/bg-12-3849-2015, 2015.

Beringer, J., Livesley, S. J., Randle, J., and Hutley, L. B.: Carbon dioxide fluxes dominate the greenhouse gas exchanges of a seasonal wetland in the wet-dry tropics of Northern Australia, Agric For Meteorol, 182–183, 239–247, https://doi.org/10.1016/j.agrformet.2013.06.008, 2013.

Bevacqua, E., Rakovec, O., Schumacher, D. L., Kumar, R., Thober, S., Samaniego, L., Seneviratne, S. I., and Zscheischler, 655 J.: Direct and lagged climate change effects intensified the 2022 European drought, Nat Geosci, 17, 1100–1107, https://doi.org/10.1038/s41561-024-01559-2, 2024.

Bhushan, A., Goyal, V. C., and Srivastav, A. L.: Greenhouse gas emissions from inland water bodies and their rejuvenation: a review, J. Water Clim. Chang, 15, 5626–5644, https://doi.org/10.2166/wcc.2024.561, 2024.

Breheny, P. and Burchett, W.: *visreg*: Visualization of regression models, R package version 2.7.0, CRAN, https://CRAN.R-660 project.org/package=visreg, 2017.

Bolker, B. M., Brooks, M. E., Clark, C. J., Geange, S. W., Poulsen, J. R., Stevens, M. H. H., and White, J. S. S.: Generalized linear mixed models: a practical guide for ecology and evolution, Trends Ecol. Evol, 24, 127–135, https://doi.org/10.1016/j.tree.2008.10.008, 2009.

Bottino, F., Souza, B. P., Rocha, R. J. S., Cunha-Santino, M. B., and Bianchini, I.: Characterization of humic substances 665 from five macrophyte species decomposed under different nutrient conditions, Limnetica, 40, 267–278, https://doi.org/10.23818/limn.40.18, 2021.

Buragienė, S., Šarauskis, E., Romaneckas, K., Adamavičienė, A., Kriaučiūnienė, Z., Avižienytė, D., Marozas, V., and Naujokienė, V.: Relationship between CO_2 emissions and soil properties of differently tilled soils, Sci. Total Environ., 662, 786–795, https://doi.org/10.1016/j.scitotenv.2019.01.236, 2019.

670   Burkett, V. and Kusler, J.: Climate change: Potential impacts and interactions in wetlands of the United States, J Am Water Resour Assoc, 36, 313–320, https://doi.org/10.1111/j.1752-1688.2000.tb04270.x, 2000.

Catalán, N., Von Schiller, D., Marcé, R., Koschorreck, M., Gomez-Gener, L., and Obrador, B.: Carbon dioxide efflux during the flooding phase of temporary ponds, Limnetica, 29, 349–360, http://doi.org/10.23818/limn.33.27, 2014.

Čížková, H., Květ, J., Comín, F. A., Laiho, R., Pokorný, J., and Pithart, D.: Actual state of European wetlands and their
675   possible future in the context of global climate change, Aquat Sci, 75, 3–26, https://doi.org/10.1007/s00027-011-0233-4, 2013.

Cole, J. J. and Caraco, N. F.: Atmospheric exchange of carbon dioxide in a low-wind oligotrophic lake measured by the addition of SF6, Limnol Oceanogr, 43, 647–656, https://doi.org/10.4319/lo.1998.43.4.0647, 1998.

Cole, J. J., Prairie, Y. T., Caraco, N. F., McDowell, W. H., Tranvik, L. J., Striegl, R. G., Duarte, C. M., Kortelainen, P.,
680   Downing, J. A., Middelburg, J. J., and Melack, J.: Plumbing the global carbon cycle: Integrating inland waters into the terrestrial carbon budget, Ecosystems, 10, 171–184, https://doi.org/10.1007/s10021-006-9013-8, 2007.

Copernicus Climate Change Service (C3S): European State of the Climate 2022, Copernicus Climate Change Service, https://climate.copernicus.eu/ESOTC/2022, 2023.

DelVecchia, A. G., Gougherty, S., Taylor, B. W., and Wissinger, S. A.: Biogeochemical characteristics and hydroperiod
685   affect carbon dioxide flux rates from exposed high-elevation pond sediments, Limnol Oceanogr, 66, 1050–1067, https://doi.org/10.1002/lno.11663, 2021.

Dimitriou, E., Moussoulis, E., Stamati, F., and Nikolaidis, N.: Modelling hydrological characteristics of Mediterranean Temporary Ponds and potential impacts from climate change, Hydrobiologia, 634, 195–208, https://doi.org/10.1007/s10750-009-9898-2, 2009.

690   Downing, J. A.: Emerging global role of small lakes and ponds: Little things mean a lot, Limnetica, 29, 9–24, https://doi.org/10.23818/limn.29.02, 2010.

Fellman, J., Hood, E., and Spencer, R.: Fluorescence spectroscopy opens new windows into dissolved organic matter dynamics in freshwater ecosystems: A review, Limnol Oceanogr, 55, 2452–2462, https://doi.org/10.4319/lo.2010.55.6.2452, 2010.

695   Fox, J.: Effect Displays in R for Generalised Linear Models, J Stat Softw, 8, 1–27, https://doi.org/10.18637/jss.v008.i15, 2003.

Fraser, F. C., Corstanje, R., Deeks, L. K., Harris, J. A., Pawlett, M., Todman, L. C., Whitmore, A. P., and Ritz, K.: On the origin of carbon dioxide released from rewetted soils, Soil Biol Biochem, 101, 1–5, https://doi.org/10.1016/j.soilbio.2016.06.032, 2016.

700   Fromin, N., Pinay, G., Montuelle, B., Landais, D., Ourcival, J. M., Joffre, R., and Lensi, R.: Impact of seasonal sediment desiccation and rewetting on microbial processes involved in greenhouse gas emissions, Ecohydrology, 3, 339–348, https://doi.org/10.1002/eco.115, 2010.

Gabor, R., Baker, A., Mcknight, D., and Miller, M.: Fluorescence Indices and Their Interpretation, in: Aquatic Organic Matter Fluorescence, edited by: Coble, P. G., Lead, J., Baker, A., Reynolds, D. M., and Spencer, R. G. M., Cambridge University Press, Cambridge, 303–338, https://doi.org/10.1017/CBO9781139045452.015, 2014.

Gao, Y., Li, J., Wang, S., Jia, J., Wu, F., and Yu, G.: Global inland water greenhouse gas (GHG) geographical patterns and escape mechanisms under different water level, Water Res., 269, 122808, https://doi.org/10.1016/j.watres.2024.122808–, 2025.

Garcia-Murillo, P., Díaz-Paniagua, C., and Fernández-Zamudio, R.: Decline of aquatic plants in an iconic European protected natural area, J Nat Conserv, 84, 126814, https://doi.org/10.1016/j.jnc.2024.126814, 2025.

Gilbert, P. J., Cooke, D. A., Deary, M., Taylor, S., and Jeffries, M. J.: Quantifying rapid spatial and temporal variations of CO_2 fluxes from small, lowland freshwater ponds, Hydrobiologia, 793, 83–93, https://doi.org/10.1007/s10750-016-2855-y, 2017.

Girard, L., Davidson, T. A., Tolon, V., Bucak, T., Rouifed, S., Wezel, A., and Robin, J.: The balance of carbon emissions versus burial in fish ponds: The role of primary producers and management practices, Aquac. Rep., 39, 102456, https://doi.org/10.1016/j.aqrep.2024.102456, 2024.

Gómez-Gener, L., Obrador, B., Marcé, R., Acuña, V., Catalán, N., Casas-Ruiz, J. P., Sabater, S., Muñoz, I., and von Schiller, D.: When Water Vanishes: Magnitude and Regulation of Carbon Dioxide Emissions from Dry Temporary Streams, Ecosystems, 19, 710–723, https://doi.org/10.1007/s10021-016-9963-4, 2016.

Gómez-Rodríguez, C., Bustamante, J., and Díaz-Paniagua, C.: Evidence of hydroperiod shortening in a preserved system of temporary ponds, Remote Sens-, 2, 1439–1462, https://doi.org/10.3390/rs2061439, 2010.

Google LLC: Google Earth Pro, https://www.google.com/earth/, 2021.

Sen Gupta, R. and Koroleff, F.: A quantitative study of nutrient fractions and a stoichiometric model of the Baltic, Estuar. Coast. Shelf Sci., 1, 335–360, https://doi.org/10.1016/0302-3524(73)90025-X, 1973.

Håkanson, L.: On the relationship between lake trophic level and lake sediments, Water Res, 18, 303–314, https://doi.org/https://doi.org/10.1016/0043-1354(84)90104-0, 1984.

Hanken, N.-M., Bjørlykke, K., and Nielsen, J. K.: Carbonate Sediments, in: Petroleum Geoscience: From Sedimentary Environments to Rock Physics, edited by: Bjørlykke, K., Springer Berlin Heidelberg, Berlin, Heidelberg, 151–216, https://doi.org/10.1007/978-3-642-34132-8_5, 2015.

Hanson, P. C., Pace, M. L., Carpenter, S. R., Cole, J. J., and Stanley, E. H.: Integrating Landscape Carbon Cycling: Research Needs for Resolving Organic Carbon Budgets of Lakes, Ecosystems, 18, 363–375, https://doi.org/10.1007/s10021-014-9826-9, 2015.

Hartig, F.: DHARMa: Residual Diagnostics for Hierarchical (Multi-Level / Mixed) Regression Models, R package version 0.4.7, CRAN, 0.32614/CRAN.package.DHARMa, -2022.

735 Heiri, O., Lotter, A. F., & Lemcke, G. Loss on ignition as a method for estimating organic and carbonate content in sediments: Reproducibility and comparability of results, J. Paleolimnol, *25*, 101–110. https://doi.org/10.1023/A:1008119611481, 2001.

Hill, M. J., Greaves, H. M., Sayer, C. D., Hassall, C., Milin, M., Milner, V. S., Marazzi, L., Hall, R., Harper, L. R., Thornhill, I., Walton, R., Biggs, J., Ewald, N., Law, A., Willby, N., White, J. C., Briers, R. A., Mathers, K. L., Jeffries, M. J.,
740 and Wood, P. J.: Pond ecology and conservation: research priorities and knowledge gaps, Ecosphere, 12, https://doi.org/10.1002/ecs2.3853, 2021.

Holgerson, M. A. and Raymond, P. A.: Large contribution to inland water CO_2 and CH_4 emissions from very small ponds, Nat Geosci, 9, 222–226, https://doi.org/10.1038/ngeo2654, 2016.

Huguet, A., Vacher, L., Relexans, S., Saubusse, S., Froidefond, J. M., and Parlanti, E.: Properties of fluorescent dissolved
745 organic matter in the Gironde Estuary, Org Geochem, 40, 706–719, https://doi.org/https://doi.org/10.1016/j.orggeochem.2009.03.002, 2009.

IPCC: Climate change 2014: synthesis report, edited by: Contribution of working Groups I, II and III to the fifth assessment report of the I. P. on C. C., Geneva, 2014.

Jarvis, P., Petsikos, C., Wingate, L., Rayment, M., Pereira, J., Banza, J., David, J., Miglietta, F., Borghetti, M., Manca, G.,
750 and Valentini, R.: Drying and wetting of Mediterranean soils stimulates decomposition and carbon dioxide emission: The "Birch effect," Tree Physiol, 27, 929–940, https://doi.org/10.1093/treephys/27.7.929, 2007.

Johannesson, C. F., Nordén, J., Lange, H., Silvennoinen, H., and Larsen, K. S.: Optimizing the closure period for improved accuracy of chamber-based greenhouse gas flux estimates, Agric. For. Meteorol., 359, 110289, https://doi.org/10.1016/j.agrformet.2024.110289, 2024.

755 Kahle, D. and Wickham, H.: ggmap: Spatial Visualization with ggplot2, R package version 3.0.2, CRAN, 10.32614/CRAN.package.ggmap, 2023.

Kassambara, A.: rstatix: Pipe-Friendly Framework for Basic Statistical Tests, R package version 0.7.2, CRAN, 10.32614/CRAN.package.rstatix, 2023.

Keller, P. S., Catalán, N., von Schiller, D., Grossart, H. P., Koschorreck, M., Obrador, B., Frassl, M. A., Karakaya, N.,
760 Barros, N., Howitt, J. A., Mendoza-Lera, C., Pastor, A., Flaim, G., Aben, R., Riis, T., Arce, M. I., Onandia, G., Paranaíba, J. R., Linkhorst, A., del Campo, R., Amado, A. M., Cauvy-Fraunié, S., Brothers, S., Condon, J., Mendonça, R. F., Reverey, F., Rõõm, E. I., Datry, T., Roland, F., Laas, A., Obertegger, U., Park, J. H., Wang, H., Kosten, S., Gómez, R., Feijoó, C., Elosegi, A., Sánchez-Montoya, M. M., Finlayson, C. M., Melita, M., Oliveira Junior, E. S., Muniz, C. C., Gómez-Gener, L., Leigh, C., Zhang, Q., and Marcé, R.: Global CO_2 emissions from dry inland waters share common drivers across
765 ecosystems, Nat Commun, 11, https://doi.org/10.1038/s41467-020-15929-y, 2020.

Lauerwald, R., Allen, G. H., Deemer, B. R., Liu, S., Maavara, T., Raymond, P., Alcott, L., Bastviken, D., Hastie, A., Holgerson, M. A., Johnson, M. S., Lehner, B., Lin, P., Marzadri, A., Ran, L., Tian, H., Yang, X., Yao, Y., and Regnier, P.:

Inland Water Greenhouse Gas Budgets for RECCAP2: 2. Regionalization and Homogenization of Estimates, Global Biogeochem Cycles, 37, https://doi.org/10.1029/2022GB007658, 2023.

770 Jin, X., Wu, F., Wu, Q., Heděnec, P., Peng, Y., Wang, Z., & Yue, K.: Effects of drying-rewetting cycles on the fluxes of soil greenhouse gases. Heliyon, 9(1). https://doi.org/10.1016/j.heliyon.2023.e12984, 2023.

Lee, S.-Y., Ryan, M. E., Hamlet, A. F., Palen, W. J., Lawler, J. J., and Halabisky, M.: Projecting the Hydrologic Impacts of Climate Change on Montane Wetlands, PLoS One, 10, e0136385-, https://doi.org/10.1371/journal.pone.0136385, 2015.

Lellei-Kovács, E., Kovács-Láng, E., Botta-Dukát, Z., Kalapos, T., Emmett, B., and Beier, C.: Thresholds and interactive

775 effects of soil moisture on the temperature response of soil respiration, Eur J Soil Biol, 47, 247–255, https://doi.org/10.1016/j.ejsobi.2011.05.004, 2011.

Lenth, R. V.: emmeans: Estimated Marginal Means, aka Least-Squares Means, R package version 1.8.9, CRAN, 10.32614/CRAN.package.emmeans, 2025.

Lloyd, J. and Taylor, J. A.: On the Temperature Dependence of Soil Respiration, Funct Ecol, 8, 315–323,

780 https://doi.org/10.2307/2389824, 1994.

López-de Sancha, A., Benejam, L., Boix, D., Briggs, L., Cuenca-Cambronero, M., Davidson, T. A., De Meester, L., Fahy, J. C., Lemmens, P., Martin, B., Mehner, T., Oertli, B., Rasmussen, M., Greaves, H. M., Sayer, C., Beklioğlu, M., Brys, R., and Brucet, S.: Drivers of amphibian species richness in European ponds, Ecography, https://doi.org/10.1111/ecog.07347, 2025a.

López-de Sancha, A., Boix, D., Benejam, L., Briggs, L., Davidson, T. A., Fahy, J. C., Frutos-Aragón, V., Greaves,

785 H. M., Lemmens, P., Mehner, T., Martín, L., Oertli, B., Sayer, C., and Brucet, S.: Amphibian conservation in Europe: the importance of pond condition, Biodivers Conserv, https://doi.org/10.1007/s10531-025-03033-w, 2025b.

Lüdecke, D.: sjPlot: Data Visualization for Statistics in Social Science, R package version 2.9.0, CRAN, 10.32614/CRAN.package.sjPlot, 2025.

Ma, J., Wang, Z. Y., Stevenson, B. A., Zheng, X. J., & Li, Y.: An inorganic CO_2 diffusion and dissolution process explains

790 negative CO_2 fluxes in saline/alkaline soils. Sci. Rep., 3, 2025, https://doi.org/10.1038/srep02025, 2013.

Madaschi, C., Cuassolo, F., Trochine, C., and Diaz-Villanueva, V.: Drivers of CO_2 fluxes in the aquatic and dry phases of Patagonian temporary wetlands, Environ. Process., 12, 1–16, https://doi.org/10.1007/s40710-025-00787-x, 2025.

Marcé, R., Obrador, B., Gómez-Gener, L., Catalán, N., Koschorreck, M., Arce, M. I., Singer, G., and von Schiller, D.:

795 Emissions from dry inland waters are a blind spot in the global carbon cycle, Earth-Sci. Rev., 188, 240–248, https://doi.org/10.1016/j.earscirev.2018.11.012, 2019.

Martinsen, K. T., Kragh, T., and Sand-Jensen, K.: Carbon dioxide fluxes of air-exposed sediments and desiccating ponds, Biogeochemistry, 144, 165–180, https://doi.org/10.1007/s10533-019-00579-0, 2019.

Morant, D., Picazo, A., Rochera, C., Santamans, A. C., Miralles-Lorenzo, J., and Camacho, A.: Influence of the conservation

800 status on carbon balances of semiarid coastal Mediterranean wetlands, Inland Waters, 10, 453–467, https://doi.org/10.1080/20442041.2020.1772033, 2020.

Murphy, K. R., Stedmon, C. A., Graeber, D., and Bro, R.: Fluorescence spectroscopy and multi-way techniques. PARAFAC, Anal. Methods, 5, 6557, https://doi.org/10.1039/c3ay41160e, 2013.

Nag, S. K., Das Ghosh, B., Nandy, S., Aftabuddin, M., Sarkar, U. K., and Das, B. K.: Comparative assessment of carbon sequestration potential of different types of wetlands in lower Gangetic basin of West Bengal, India, Environ Monit Assess, 195, 154, https://doi.org/10.1007/s10661-022-10729-x, 2023.

Novikmec, M., Hamerlík, L., Kočický, D., Hrivnák, R., Kochjarová, J., Oťaheľová, H., Paľove-Balang, P., and Svitok, M.: Ponds and their catchments: size relationships and influence of land use across multiple spatial scales, Hydrobiologia, 774, 155–166, https://doi.org/10.1007/s10750-015-2514-8, 2016.

Obrador, B., Von Schiller, D., Marcé, R., Gómez-Gener, L., Koschorreck, M., Borrego, C., and Catalán, N.: Dry habitats sustain high CO_2 emissions from temporary ponds across seasons, Sci Rep, 8, 3015, https://doi.org/10.1038/s41598-018-20969-y, 2018.

Oertel, C., Matschullat, J., Zurba, K., Zimmermann, F., and Erasmi, S.: Greenhouse gas emissions from soils—A review, Chem. Erde, 76, 327–352, https://doi.org/10.1016/j.chemer.2016.04.002, 2016.

Oertli, B., Céréghino, R., Hull, A., and Miracle, R.: Pond conservation: From science to practice, Hydrobiologia, 634, 1–9, https://doi.org/10.1007/s10750-009-9891-9, 2009.

Oroud, I. M.: The implications of climate change on freshwater resources in the arid and semiarid Mediterranean environments using hydrological modeling, GIS tools, and remote sensing, Environ Monit Assess, 196, 979, https://doi.org/10.1007/s10661-024-13139-3, 2024.

Page, K. L. and Dalal, R. C.: Contribution of natural and drained wetland systems to carbon stocks, CO_2, N_2O, and CH_4 fluxes: An Australian perspective, Soil Res., 49, 377–388, https://doi.org/10.1071/SR11024, 2011.

Pekel, J.-F., Cottam, A., Gorelick, N., and Belward, A. S.: High-resolution mapping of global surface water and its long-term changes, Nature, 540, 418–422, https://doi.org/10.1038/nature20584, 2016.

Petersen, S. O., Hoffmann, C. C., Schäfer, C. M., Blicher-Mathiesen, G., Elsgaard, L., Kristensen, K., Larsen, S. E., Torp, S. B., and Greve, M. H.: Annual emissions of CH_4 and N_2O, and ecosystem respiration, from eight organic soils in Western Denmark managed by agriculture, Biogeosciences, 9, 403–422, https://doi.org/10.5194/bg-9-403-2012, 2012.

Peterson, R. A. and Cavanaugh, J. E.: Ordered quantile normalization: a semiparametric transformation built for the cross-validation era, J Appl Stat, 47, 2312–2327, https://doi.org/10.1080/02664763.2019.1630372, 2020.

Pickens, A. H., Hansen, M. C., Hancher, M., Stehman, S. V., Tyukavina, A., Potapov, P., Marroquin, B., and Sherani, Z.: Mapping and sampling to characterize global inland water dynamics from 1999 to 2018 with full Landsat time-series, Remote Sens Environ, 243, 111792, https://doi.org/10.1016/j.rse.2020.111792, 2020.

Podgrajsek, E., Sahlée, E., Bastviken, D., Holst, J., Lindroth, A., Tranvik, L., & Rutgersson, A.: Comparison of floating chamber and eddy covariance measurements of lake greenhouse gas fluxes. Biogeosciences, 11, 4225–4233. https://doi.org/10.5194/bg-11-4225-2014.

835 Pozzo-Pirotta, L. J., Montes-Pérez, J. J., Sammartino, S., Marcé, R., Obrador, B., Escot, C., Reyes, I., and Moreno-Ostos, E.: Carbon dioxide emission from drawdown areas of a Mediterranean reservoir, Limnetica, 41, 61–72, https://doi.org/10.23818/limn.41.05, 2022.

Prananto, J. A., Minasny, B., Comeau, L. P., Rudiyanto, R., and Grace, P.: Drainage increases CO_2 and N_2O emissions from tropical peat soils, Glob Chang Biol, 26, 4583–4600, https://doi.org/10.1111/gcb.15147, 2020.

840 Premke, K., Attermeyer, K., Augustin, J., Cabezas, A., Casper, P., Deumlich, D., Gelbrecht, J., Gerke, H. H., Gessler, A., Grossart, H. P., Hilt, S., Hupfer, M., Kalettka, T., Kayler, Z., Lischeid, G., Sommer, M., and Zak, D.: The importance of landscape diversity for carbon fluxes at the landscape level: small-scale heterogeneity matters, Wiley Interdisciplinary Reviews: Water, 3, 601–617, https://doi.org/10.1002/wat2.1147, 2016.

Pucher, M., Wünsch, U., Weigelhofer, G., Murphy, K., Hein, T., and Graeber, D.: StaRdom: Versatile software for analyzing
845 spectroscopic data of dissolved organic matter in R, Water, 11, 2366, https://doi.org/10.3390/w11112366, 2019.

R Core Team: R: A language and environment for statistical computing, R Foundation for Statistical Computing, Vienna, Austria, https://www.R-project.org/, 2024.

Raymond, P. A., Hartmann, J., Lauerwald, R., Sobek, S., McDonald, C., Hoover, M., Butman, D., Striegl, R., Mayorga, E., Humborg, C., Kortelainen, P., Dürr, H., Meybeck, M., Ciais, P., and Guth, P.: Global carbon dioxide emissions from inland
850 waters, Nature, 503, 355–359, https://doi.org/10.1038/nature12760, 2013.

Rey, A.: Mind the gap: Non-biological processes contributing to soil CO_2 efflux, Glob. Change Biol., 21, 1752–1761, https://doi.org/10.1111/gcb.12821, 2015.

Roland, M., Serrano-Ortiz, P., Kowalski, A. S., Goddéris, Y., Sánchez-Cañete, E. P., Ciais, P., Domingo, F., Cuezva, S., Sanchez-Moral, S., Longdoz, B., Yakir, D., Van Grieken, R., Schott, J., Cardell, C., and Janssens, I. A.: Atmospheric
855 turbulence triggers pronounced diel pattern in karst carbonate geochemistry, Biogeosciences, 10, 5009–5017, https://doi.org/10.5194/bg-10-5009-2013, 2013.

Rulík, M., Weber, L., Min, S., and Šmíd, R.: CO_2 and CH_4 fluxes from inundated floodplain ponds: role of diel variability and duration of inundation, Front Environ Sci, 11, https://doi.org/10.3389/fenvs.2023.1006988, 2023.

Ryan A. Peterson: Finding Optimal Normalizing Transformations via bestNormalize, R J, 13, 310–329,
860 https://doi.org/10.32614/RJ-2021-041, 2021.

Sabater, S., Timoner, X., Borrego, C., and Acuña, V.: Stream biofilm responses to flow intermittency: From cells to ecosystems, Front Environ Sci, 4, https://doi.org/10.3389/fenvs.2016.00014, 2016.

Sala, J., Gascón, S., Boix, D., Gesti, J., and Quintana, X. D.: Proposal of a rapid methodology to assess the conservation status of Mediterranean wetlands and its application in Catalunya (NE Iberian Peninsula), Arch. Sci., 57, 123–132, 2005.

865 Sánchez-Carrillo, S.: Hydrology and biogeochemistry of Mediterranean temporary ponds, International Conference on Mediterranean Temporary Ponds. Proceedings and Abstracts, 73–82, 2009.

Semsirion AG: SCD30 CO_2 and RHT Sensor Datasheet, Version 1.0 – D1, https://sensirion.com/media/documents/4EAF6AF8/61652C3C/Sensirion_CO2_Sensors_SCD30_Datasheet.pdf, 2020.

Sponseller, R. A.: Precipitation pulses and soil CO_2 flux in a Sonoran Desert ecosystem, Glob Chang Biol, 13, 426–436, https://doi.org/https://doi.org/10.1111/j.1365-2486.2006.01307.x, 2007.

Suh, S., Lee, E., and Lee, J.: Temperature and moisture sensitivities of CO_2 efflux from lowland and alpine meadow soils, Journal of Plant Ecology, 2, 225–231, https://doi.org/10.1093/jpe/rtp021, 2009.

Tak, D. B. Y., Vroom, R. J. E., Lexmond, R., Lamers, L. P. M., Robroek, B. J. M., and Temmink, R. J. M.: Water level and vegetation type control carbon fluxes in a newly-constructed soft-sediment wetland, Wetl Ecol Manag, 31, 583–594, https://doi.org/10.1007/s11273-023-09936-1, 2023.

Taylor, S., Gilbert, P. J., Cooke, D. A., Deary, M. E., and Jeffries, M. J.: High carbon burial rates by small ponds in the landscape, Front Ecol Environ, 17, 25–31, https://doi.org/10.1002/fee.1988, 2019.

Thien, S. J.: A flow diagram for teaching texture-by-feel analysis, Journal of Agronomic Education, 8, 54–55, https://doi.org/https://doi.org/10.2134/jae.1979.0054, 1979.

Tranvik, L. J., Downing, J. A., Cotner, J. B., Loiselle, S. A., Striegl, R. G., Ballatore, T. J., Dillon, P., Finlay, K., Fortino, K., Knoll, L. B., Kortelainen, P. L., Kutser, T., Larsen, Soren., Laurion, I., Leech, D. M., McCallister, S. L., McKnight, D. M., Melack, J. M., Overholt, E., Porter, J. A., Prairie, Y., Renwick, W. H., Roland, F., Sherman, B. S., Schindler, D. W., Sobek, S., Tremblay, A., Vanni, M. J., Verschoor, A. M., von Wachenfeldt, E., and Weyhenmeyer, G. A.: Lakes and reservoirs as regulators of carbon cycling and climate, Limnol Oceanogr, 54, 2298–2314, https://doi.org/https://doi.org/10.4319/lo.2009.54.6_part_2.2298, 2009.

Unger, S., Máguas, C., Pereira, J. S., David, T. S., and Werner, C.: The influence of precipitation pulses on soil respiration - Assessing the "Birch effect" by stable carbon isotopes, Soil Biol Biochem, 42, 1800–1810, https://doi.org/10.1016/j.soilbio.2010.06.019, 2010.

Verpoorter, C., Kutser, T., Seekell, D. A., and Tranvik, L. J.: A global inventory of lakes based on high-resolution satellite imagery, Geophys Res Lett, 41, 6396–6402, https://doi.org/10.1002/2014GL060641, 2014.

Vicente-Serrano, S. M., Peña-Angulo, D., Beguería, S., Domínguez-Castro, F., Tomás-Burguera, M., Noguera, I., Gimeno-Sotelo, L., and El Kenawy, A.: Global drought trends and future projections, Philosophical Transactions of the Royal Society A: Mathematical, Physical and Engineering Sciences, 380, 20210285, https://doi.org/10.1098/rsta.2021.0285, 2022.

Voudouri, M. O., Liaskou, P., Manios, E. M., and Anagnostopoulou, C.: Top European Droughts since 1991, 94, https://doi.org/10.3390/environsciproc2023026094, 2023.

Wang, J., Song, C., Reager, J. T., Yao, F., Famiglietti, J. S., Sheng, Y., MacDonald, G. M., Brun, F., Schmied, H. M., Marston, R. A., and Wada, Y.: Recent global decline in endorheic basin water storages, Nat Geosci, 11, 926–932, https://doi.org/10.1038/s41561-018-0265-7, 2018.

Wang, M., Hao, T., Deng, X., Wang, Z., Cai, Z., and Li, Z.: Effects of sediment-borne nutrient and litter quality on macrophyte decomposition and nutrient release, Hydrobiologia, 787, 205–215, https://doi.org/10.1007/s10750-016-2961-x, 2017.

Wei, T. and Simko, V.: R package "corrplot": Visualization of a Correlation Matrix, GitHub, https://github.com/taiyun/corrplot, 2024.

Weisberg, S. and Fox, J.: Multivariate Linear Models in R, in: An R Companion to Applied Regression, Sage, Thousand
905 Oaks, CA, 2011.

Weise, L., Ulrich, A., Moreano, M., Gessler, A., E. Kayler, Z., Steger, K., Zeller, B., Rudolph, K., Knezevic-Jaric, J., and Premke, K.: Water level changes affect carbon turnover and microbial community composition in lake sediments, FEMS Microbiol Ecol, 92, fiw035, https://doi.org/10.1093/femsec/fiw035, 2016.

Weishaar, J. L., Aiken, G. R., Bergamaschi, B. A., Fram, M. S., Fujii, R., and Mopper, K.: Evaluation of Specific Ultraviolet
910 Absorbance as an Indicator of the Chemical Composition and Reactivity of Dissolved Organic Carbon, Environ Sci Technol, 37, 4702–4708, https://doi.org/10.1021/es030360x, 2003.

Wickham, H.: ggplot2: Elegant Graphics for Data Analysis, 2nd Edn., Springer, Cham, https://doi.org/10.1007/978-3-319-24277-4, 2016.

Williams, A., Williams, P., Biggs, J., Fox, G., Nicolet, P., Whitfierld Williams, M. P., Biggs, J., Fox, G., Nicolet, P., and
915 Whitfield, M.: History, origins and importance of temporary ponds Item Type article History, Origins And Importance Of Temporary Ponds, Freshwater Forum, 17, 1–10, 2010.

Wouters, H.: Downscaled bioclimatic indicators for selected regions from 1978 to 2018 derived from reanalysis, Copernicus Climate Data Store (CDS), ERA5, https://cds.climate.copernicus.eu/datasets/sis-biodiversity-era5-regional, accessed on 01-Jun-2023, 2021.

920 Zhao, M., Han, G., Li, J., Song, W., Qu, W., Eller, F., Wang, J., and Jiang, C.: Responses of soil CO_2 and CH_4 emissions to changing water table level in a coastal wetland, J Clean Prod, 269, 122316, https://doi.org/10.1016/j.jclepro.2020.122316, 2020.

Zou, J., Ziegler, A. D., Chen, D., McNicol, G., Ciais, P., Jiang, X., Zheng, C., Wu, J., Wu, J., Lin, Z., He, X., Brown, L. E., Holden, J., Zhang, Z., Ramchunder, S. J., Chen, A., and Zeng, Z.: Rewetting global wetlands effectively reduces major
925 greenhouse gas emissions, Nat Geosci, 15, 627–632, https://doi.org/10.1038/s41561-022-00989-0, 2022.